SHORT THESIS FOR THE DEGREE OF DOCTOR OF PHILOSOPHY (PHD)

Design and Development of a New Hand and Wrist Rehabilitation Robot-Assisted System; Equipped With Game-Based Therapy, ROM and Tip-Pinch Force Self-Assessment Approaches

By: Husam AbdulKareem ALmusawi

Supervisor: Dr Husi Géza

UNIVERSITY OF DEBRECEN

DOCTORAL SCHOOL OF INFORMATICS

Debrecen, 2021

Table of Contents

Chapter 1: INTRODUCTION

The hand is one of the foremost vital limbs of humans; it is a multi-fingered extremity at the end of the arm. It consists of five fingers and a wrist. It is one means by which humans have changed the world by creating gigantic buildings and machines. Human hands are an influential part of the human body since they are extraordinarily mobile and can execute a delicate and extensive range of duties, covering activity of daily living (ADL) (e.g., gripping different objects, holding things, transporting, moving, writing, eating, touching, and even changing the world). Unfortunately, many conditions, including stroke, spinal cord injury, tendon shatters, and fall-related injuries, can lead to the impairment of hand motor and sensorimotor functions of the upper extremity (UE). Approximately 80% stroke or Cerebral vascular accidents survivors develop hemiparesis in the upper arm, the dominant symptom of which is an inability to grasp an object [1]. Moreover, Stroke is also the second-leading cause of mortality worldwide [2]. It is estimated that over 15 million people each year have a stroke over the world. There are five million deaths and another five million who are permanently incapacitated due to their motor disability [3]. The majority of them will necessitate care and neurorehabilitation [4]. This process called rehabilitation Which helps re-learning of movement [5]. Neuroplasticity, also termed Neuroplasticity, is a concept that claims that neurons can form new connections through the repetition of learning and experience [6]. The goal of rehabilitation is to restructure and reinvigorate the neuronal connections in these motor patterns that were destroyed due to disease or an accident, with a detrimental impact on patients' upper limbs. These help individuals who survived to deal with their disabilities. Physio-therapists aid patients in regaining lost abilities during conventional rehabilitation, these approaches draw upon methods and approaches similar to physical therapy, which works to restore motion and exercise, as well as occupational therapy, which works to teach patients how to do their daily routines, including eating, drinking, and personal care. Current medical evidence and Rehabilitation care recommendations are suggesting that patients receive care for brain injury as soon as possible [7].

However, it is important to identify possible obstacles, as well as possible advantages, because recovery of upper extremity functions may be limited as well as further hampered by the lack of available resources. (e.g., enough trained physiotherapist, facilities) which is further complicated problem. While physiotherapy appointments with professionals do allow only a limited number

of exercises, unfortunately, this is often due to scheduling constraints and patient preference. Usually, the therapist starts with the primary focus to rehabilitate the lower extremity to help victims regain their balance and mobility, which usually leads to neglect of the UE, putting the stroke victims at a greater risk of hand and arm disability. Due to the rising number of patients, there are not enough resources to treat them with traditional methods, making those methods costly and hard to handle. These facts lead to the majority of stroke patients not receiving sufficient treatment, and according to statistics, only approximately 12% of stroke patients show a considerable improvement in their capability to use their upper limbs [8].

Therefore, there is a critical need to develop technologies that can relieve the burden on health professionals, provide the necessary active and passive exercises, motivate the patients, contribute to strengthening the active range of motion AROM, and grasp force.

Over the last years, the researchers came up with various ergonomically strategies by combining the power of robotic technology with sophisticated medical therapies to work hand in hand.

The robot-assisted rehabilitation devices are a mechatronic device in which a specially designed external mechanism is coupled to the individual body and deliver a necessary force to perform the required gestures of the human limb. These assistive motions can be formed with different modes, including active, passive, Continuous Passive Motion (CPM), and interactive modes. Moreover, these devices then transfer the generated motion link to the affected limb, depending on the mechanical structure and the diver transmission mechanism.

A significant advancement in conventional recovery approaches has contributed to assistive robotics. Assistive rehabilitation robotic has progressed and increased the human quality of life significantly. Increasing emphasis was given to technical advances in robotics during refurbishment training [9], [10]. Additionally, it should be noted that these therapeutic robotics are not meant to replace therapists; their purpose is to assist the time-consuming, and challenging task therapists must conduct. [11], [12].

Additionally, numerous considerations should be taken in mind when designing robot-assisted rehabilitation that integrates directly with the human body, such as strike technical and clinical requirements. Additionally, the human hands represent a higher challenge to the invention of robotics that integrates with it

because of their complex anatomy shape, since the designers must follow this complexity.

1.1. AIMS AND OBJECTIVES

The primary goal of this dissertation is to demonstrate a novel design and development of self-assessment fingers, and wrist rehabilitation mechatronic system to aid with the recovery progress of survivors who suffer hemiparesis of the upper arm caused by brain injury, spinal cord injury, tendon shatters, or fall-related injuries. The aimed system step forward to improve the related existing devices. The objective of the proposed system to help the users regain both right and/or left-hand functionality and sensory motor and reduce spasticity, muscle tone on the hand, and observe and evaluate their recovery steps. The intended system designed to be a single device that capable of performing the basic movements of the hand movement, including one fingers flexion/ Extension (F/E) including the thumb (F/E); plus, two wrist movements wrist flexion/ Extension (F/E), and Wrist Radial/ulnar (R/U) deviation; and one forearm pronation/supination (P/S). Additional benefits of this project include helping to minimize the overall cost of rehabilitation and providing a better solution for the market, besides the proposed system aimed to develop a game-based therapy that motivates the patients during their active therapy. A self-assessment feature was considered during software development to evaluate the rehabilitation progress at the end of each therapy session. Including all these characteristics will give more people easier access towards a creative and cost-effective approach to exercise rehabilitation.

1.2. Methodology

As Figure 1 summarized the development steps, the following phases will be used to execute the methodology to accomplish the proposed development:

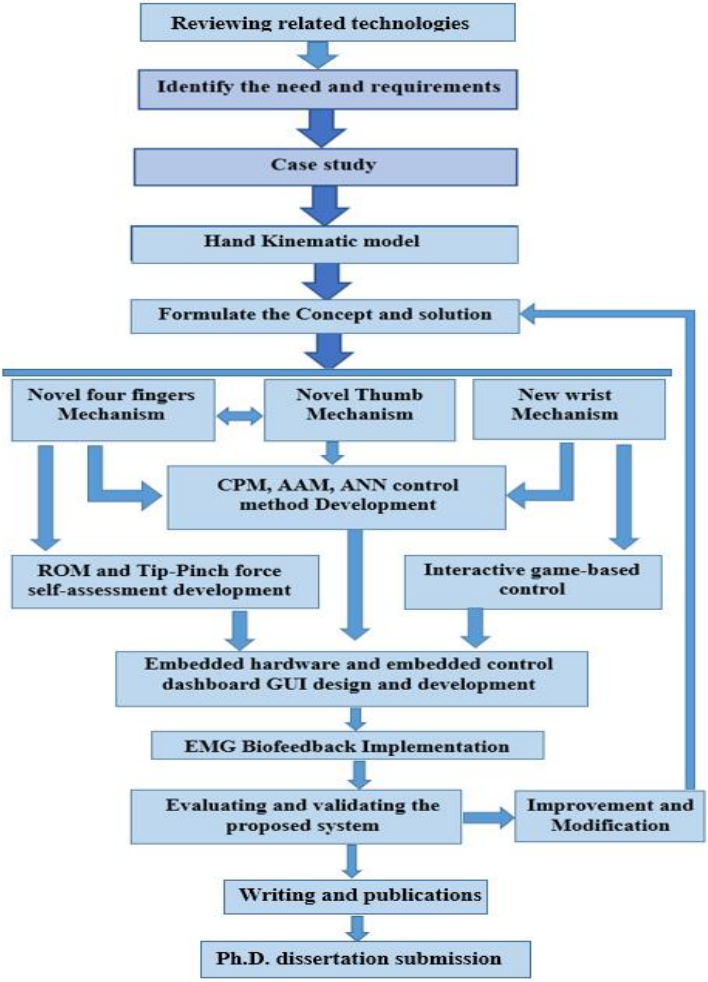

Figure 1: summarized diagram of the working process

Thesis I: Related publications: [P5, P8, P14]

- **This thesis shaped a comprehensive guideline for building robot-based hand rehabilitation for people with brain injury, Neuroplasticity, spinal cord injury, tendon shatters, or fall-related**

injuries. Since there are no proper guidelines in literature could be found. Therefore, we set and defined proper guidance towards the existing state-of-the-art related technologies, and it identified the technical and clinical requirements towards design and inventing Robot-Assisted.

- **This thesis identified a clinical case study that contributes to investigating and determining the level of the impact that the stroke can cause to the hand and wrist movements and force. It also helps examine the actual cases to which helped to achieve the proper design at the Neurology and Rehabilitation department/university of Debrecen.**

Chapter 2: Background and case study

2.1. Background Summary

Although, a set of assistive-robots rehabilitation systems has been developed. Nevertheless, there are numerous limitations in the existed hand rehabilitation approaches; most of them are very expensive for local rehabilitation centres, heavy-weighted, complex structured, noisy, too challenging to operate, and too many mechanical parts linked to the patients' arms can be unconformable to both therapists and patients. In addition, specific devices are a static platform and intended for some specific applications and specific hand and joints and neglecting the thumb and the wrist from their designs. Furthermore, many existing devices control over an external PC without embedded control implementation. Besides, most of the existing solutions are not outfitted with an automated diagnostic system, self-assessment and feedback system interactive game, and a gripping force measurement instrument. All work together to facilitate accurate patient feedback and continuous motivation

throughout a long repetitive rehabilitation process. Taken together, these facts show that worldwide stroke overall survival is rising, and the death rate is climbing, which indicates a necessity towards greater and improved therapeutic facilities in the future. Therefore, considering all these limitations along with technical and clinical requirements, the proposed system also intended to step forward of improving the existing solution, this thesis describes a novel system that is capable of rehabilitating four fingers and thumb plus the wrist joints in one device, along with the process of mechanical, electronic design, and software design and development. Theoretically, the human fingers were modelled as kinematic objects and direct measurements regarding their AROM, and grabbing force was made from stroke survivors to better understand the problem. The proposed system takes advantage of the combination ground-exoskeleton and end-effector mechanism to provide the desired motions to the desired joints. The concept and the design of the proposed system were developed at Debrecen University with respect to the technical and strict clinical requirements. The system is designed for research investigations and prototyping with the help of rehabilitation practitioners. Furthermore, essential to notice, the result of this project will be a product, not medication or a surgical procedure.

The proposed system planned to target four extensional movements of the hand, which are including one fingers flexion/ Extension (F/E), two wrist movements, flexion deviation; forearm pronation/supination (P/S) These motions Figure 2 are critical for conducting activities of daily living (ADL) as instructed by therapists.

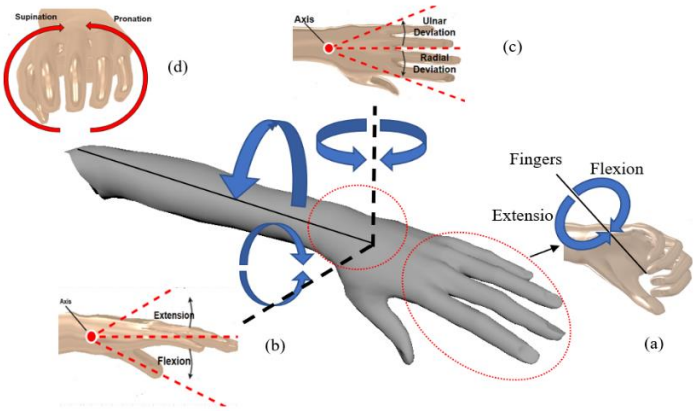

Figure 2: trainable Human Hand Motion (DOF) by the proposed system

2.2. Biomechanical Constraints Based on the Case Study: (Parameterization)

To satisfy the design concerns as it is the first step towards the objective. A case study is being conducted on stroke patients getting treatment from the Clinic of the University of Debrecen in Hungary rehabilitation department of the University of Debrecen Clinic (Figure 3). The aim is to identify the hand kinematics and associated trajectories for investigating the appropriate required data to make the target device. It was difficult to find the reference values from the literature analysis due to the inconsistency of data.

Fig[illegible] measurement by the Goniometer provided by the Rehabilitation Department

The study is seeking to investigate and determine the level of the impact that the stroke can cause to the hand and wrist movements and force. It aims to select

the right specifications for the planned device, such as the interaction force that will be induced by the proposed system towards the patient's fingers. Ten stroke patients were selected, Figure 4, shows the comparative result for two subjects only for simplicity. It is observable the difference of the grabbing force (Kg) between the two hands

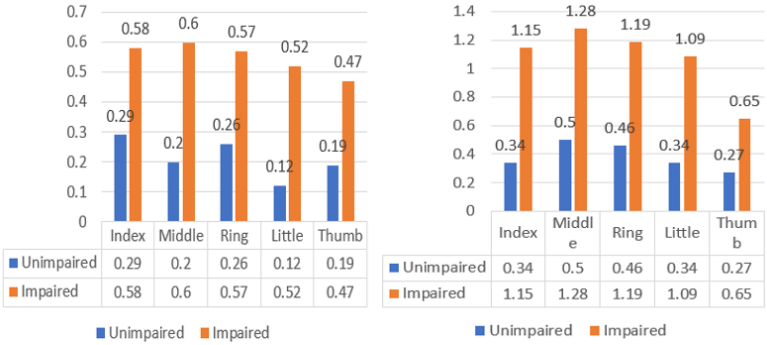

Figure 4: Measured grabbing force values (the unit of the values is Kg) of the impaired and unimpaired hand of and Subject 1 Subject 2

Additionally, the feasibility study is based on the scales given for Range of Motion (ROM) for measuring the patients impaired and unimpaired hand range of motion and Modified Ashworth Scale (MAS) for obtaining wrist and finger spasticity.

In contrast, Table 1, 2 demonstrate the measured wrist angle dorsiflexion (UP), palmer flexion (DOWN), radial deviation (LEFT) and ulnar deviation (RIGHT) is measured in degrees. The spasticity of the wrist and fingers is graded by the Modified Ashworth Scale (MAS) [13]; this six-fold scale ranges from 0 (No Spasticity) to 4 (fixed muscle contracture) by a professional physiotherapist.

Table 1: Measured values of the fingers of Impaired hand and Wrist

	Sub 1	**Sub 2**	**Sub 3**	**Sub 4**	**Sub 5**	**Sub 6**	**Sub 7**	**Sub 8**	**Sub 9**	**Sub 10**
Wrist										

MAS score of Wrist (0-4)	1	0	1		0	2	1	0	3	2
MAS score of Finger (0-4)	0	0	1		0	1+	0	0	2	1
Wrist Angle (Degrees) Up (Dorsiflexion)	12°	70°	50°	0°	60°	25°	12°	0°	22°	3°
Down (Palmer Flexion)	63°	100°	53°	80°	40°	77°	43°	80°	40°	70°
Right (Ulnar Deviation)	3°	30°	25°	10°	40°	20°	30°	0°	5°	31°
Left (Radial Deviation)	6°	30°	30°	10°	30°	30°	20°	0°	3°	12°

Table 2: Measured values of the fingers of unimpaired hand and Wrist

	Sub 1	**Sub 2**	**Sub 3**	**Sub 4**	**Sub 5**	**Sub 6**	**Sub 7**	**Sub 8**	**Sub 9**	**Sub 10**
	Wrist									
MAS score of Wrist (0-4)	0	0	0	0	0	0	0	0	0	0

MAS score of Finger (0-4)		0	0	0	0	0	0	0	0	0	0
Wrist Angle (Degrees)	Up (Dorsiflexion)	55°	110°	63°	80°	50°	30°	15°	16°	62°	72°
	Down (Palmer Flexion)	110°	70°	70°	80°	70°	80°	20°	83°	70°	90°
	Right (Ulnar Deviation)	33°	50°	53°	30°	55°	30°	40°	20°	34°	40°
	Left (Radial Deviation)	33°	52°	42°	30°	54°	24°	19°	13°	20°	40°

Thesis II: Related publications: [P2, P3, P5]

- **This thesis developed a new kinematic model for single finger F/E, thumb F/E, and Ab/Ad. We have conducted several point-to-point motions for the index finger. These movements are a decent approximation of general finger F/E gestures with 3d model representation. These analyses of the hand movement configurations are needed so that a robotic system could be able to mimic its natural movement. Besides, a 2D Index finger workspace was driven to estimate the working area of the proposed system.**

- **This thesis introduces a new exoskeleton finger-guide design with initial fingers assist-robot system design; the initial proposed design drives the end-effector of the fingers (distal phalanx) with only one MC. This hygienic solution can guide each finger independently to the desired trajectories by integrating with the distal phalanx of the targeted finger without the need to actuate PIP and MCP joints.**

Chapter 3: Human finger kinematic Model and Finger's Trajectory determining

3.1. Introduction

The human hand has many DoF compacted within a much smaller region, making it a tough challenge to simulate. The index and pinkie, middle, and ring fingers follow the exact mechanism of flexing and extending. The thumb will be modelled too since the thumb has its own mechanism. These models will be simulated using MATLAB software and its plugin called Peter Corke pagcke.
This is a 3D-dimensional kinematic model of hand finger model that includes a single finger F/E. and the thumb F/A, and Ab/Ad.

3.2. Kinematics of Index and Thumb

of the index finger representation. Figure 5(a), depicts the kinematic model of the index finger as well as the coordinate frames. While Figure 5(b), shows the proposed model considered the thumb as two links. And one active revolute joint (1 DOF for each) and one Universal joint (2DOF). Which is associated with the natural movements of the thumb including thumb F/E. The model equations are calculated using Denavit-H for the F/E in the index fingers.

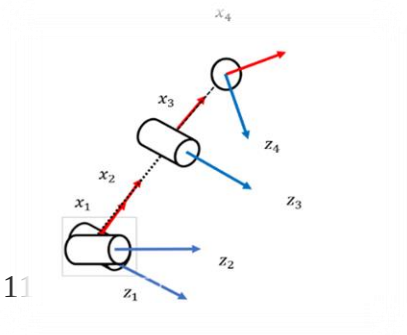

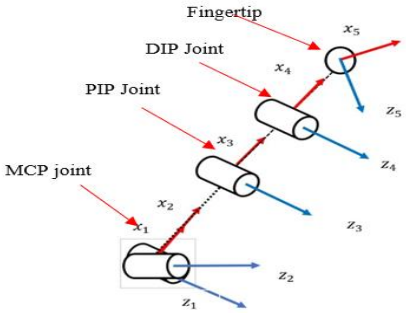

Figure 5: representation of the coordinate frame of the three-link index, (b) representation of the coordinate frame of the two-link thumb

To solve the kinematics, a theory of robotics was employed in conjunction with the theory of movement to describe four degrees of freedom in the index finger [14]. Since each joint connects two links, an N-joint finger manipulator will have an N+1 link. Whereas the link was numbered from 0 to n starting from the base, the joint was numbered from 1 to n. Thus, the joint I links link i-1 to link I, and joint i-1 moves link i. Link 0, the first link, cannot move while the joint is activated since it is attached to the ground.

Ti can get depend on four primary transformations:

$$T_i = Rot(z,\theta_i)\, Trans(z,d_i) Trans(x,a_i) Rot(x,\alpha_i) \qquad Eq\ 1$$

So, we can transfer from i frame to i+1 frame

$Rot(x,\alpha_i)$: Rotation around x axes a_i angle.

$Trans(x,a_i)$: Transformation x axes a_i angle.

$Rot(z,\theta_i)$: Rotation around z axes θ_i angle.

$Trans(z,d_i)$: Transformation z axes d_i angle.

T_i The final matrix will be the result of multiple of those matrixes.

$$T_i = \begin{bmatrix} c_{\theta i} & -s_{\theta i} & 0 & 0 \\ s_{\theta i} & c_{\theta i} & 0 & 0 \\ 0 & 0 & 1 & 0 \\ 0 & 0 & 0 & 1 \end{bmatrix} \cdot \begin{bmatrix} 1 & 0 & 0 & 0 \\ 0 & 1 & 0 & 0 \\ 0 & 0 & 1 & d_i \\ 0 & 0 & 0 & 1 \end{bmatrix} \cdot \begin{bmatrix} 1 & 0 & 0 & a_i \\ 0 & 1 & 0 & 0 \\ 0 & 0 & 1 & 0 \\ 0 & 0 & 0 & 1 \end{bmatrix} \cdot \begin{bmatrix} 1 & 0 & 0 & 0 \\ 0 & c_{\alpha i} & -s_{\alpha i} & 0 \\ 0 & s_{\alpha i} & c_{\alpha i} & 0 \\ 0 & 0 & 0 & 1 \end{bmatrix}$$

$$T_i = \begin{bmatrix} c_{\theta i} & -s_{\theta i}c_{\alpha i} & s_{\theta i}s_{\alpha i} & a_i c_{\theta i} \\ s_{\theta i} & c_{\theta i}c_{\alpha i} & -c_{\theta i}s_{\alpha i} & a_i s_{\alpha i} \\ 0 & s_{\alpha i} & c_{\alpha i} & d_i \\ 0 & 0 & 0 & 1 \end{bmatrix} \qquad Eq\ 2$$

From Eq 2 $\alpha_i, \theta_i, d_i, a_i$

a_i: The distance between z_i to z_{i+1} along the x_i axis.
α_i: The angle between z_i to z_{i+1} about x_i axis.
d_i: The distance between x_i to x_{i+1} along the z_i axis.
θ_i: The angle between x_i to x_{i+1} about z_i axis.

3.2.1. Homogeneous transformation

$H = Rot_{x,\alpha}\ \ Trans_{x,a}\ Trans_{\ z,d}\ Rot_{z,\theta}$

The homogeneous transformation H can be driven throughout rotate α angle about α axis, then translation among x axis then translation among z axis, and finally rotate θ angle about z axis.

$$H = \begin{bmatrix} c_\theta & -s_\theta & 0 & a \\ c_\alpha s_\theta & c_\theta c_\alpha & -s_\alpha & -ds_\alpha \\ s_\alpha s_\theta & s_\alpha c_\theta & c_\alpha & dc_\alpha \\ 0 & 0 & 0 & 1 \end{bmatrix} \qquad Eq\ 3$$

The homogeneous that given by this matrix is a special status and to generalize it. It should be taken into consideration that the Scale Factor= 1 and Perspective Transformation=[0 0 0].
So, the final matrix will be

$$H = \begin{bmatrix} R_{3x3} & d_{3x1} \\ f_{1x3} & S_{1x1} \end{bmatrix} = \begin{bmatrix} Rotation & Translation \\ Perspective & Scale\ factor \end{bmatrix}$$

$$H = \begin{bmatrix} \mu_x & O_x & \alpha_x & p_x \\ \mu_y & O_y & \alpha_y & p_y \\ \mu_z & O_z & \alpha_z & p_z \\ 0 & 0 & 0 & 1 \end{bmatrix}$$

Then, forward kinematics given by multiply all transforming matrixes together

$$T_i^j = T_{j+1}^j \dots\dots T_i^{i-1} \qquad Eq\ 4$$

We will use homogeneous transformation T_i^{i-1} which transfer us from i frame to i-1 frame.

$T_i^{i-1} = T_i^{i-1}(q_i)$

Depending on previous equation, the matrix $T_i^j (i > j)$

Will transfer us from i frame to j frame given by

$T_n^0 = \begin{bmatrix} R_n^0 & d_n^0 \\ 0 & 1 \end{bmatrix}$

the position and direction for the end-effector given by

$$T_n^0(q_1, q_2, \dots, q_n) = T_1^0\,(q_1).T_2^1(q_2).\dots.T_n^{n-1}(q_n)$$

$$T_i^j = T_{j+1}^j \dots T_i^{i-1} = \begin{bmatrix} R_i^j & d_i^j \\ 0 & 1 \end{bmatrix}$$

The following Table 3 below show the derived D-H convention parameters used to create the index finger model; these parameters allow for obtaining the forward kinematics model.

Table 3: DH Parameters (Index finger)

i	θ_{i-1}	d_{i-1}	a_i	α_i
1	$\boldsymbol{\theta_1}$	0	$L0$	0
2	$\boldsymbol{\theta_2}$	0	0	90°
3	$\boldsymbol{\theta_3}$	0	L1	90°
4	$\boldsymbol{\theta_4}$	0	L2	0
5	0	0	L3	0

3.2.2. *Hand Kinematic: Forward kinematics*

For hand kinematics, we study only the forward kinematics since it is enough for this thesis and project scope. Generally, the difficulty is with the forward kinematics of the robot manipulator and how the tool or end-effector positions and orientations. On other words, the forward kinematics model shows the fingertip positions and orientations once the model provides the known or estimated angles of the finger joints ($\boldsymbol{\theta_1}. . . \boldsymbol{\theta_5}$). Which referred to as global coordinates.

Where

a_i: The distance between z_i to z_{i+1} along the x_i Axis.

α_i: The angle between z_i to z_{i+1} about x_i axis.

d_i: The distance between x_i to x_{i+1} along the z_i Axis.

θ_i: The angle between x_i to x_{i+1} about z_i axis.

But applying eq3 and eq4 the matrix for each link

$$A1 = T_1^0 = \begin{bmatrix} \cos(th1) & -\sin(th1) & 0 & L0 * \cos(th1) \\ \sin(th1) & \cos(th1) & 0 & L0 * \sin(th1) \\ 0 & 0 & 1 & 0 \\ 0 & 0 & 0 & 1 \end{bmatrix} \quad \text{Eq 5}$$

$$A2 = T_2^1 = \begin{bmatrix} cos(th2) & 0 & sin(th2) & 0 \\ sin(th2) & 0 & -cos(th2) & 0 \\ 0 & 1 & 0 & 0 \\ 0 & 0 & 0 & 1 \end{bmatrix} \quad Eq\ 6$$

$$A3 = T_3^2 = \begin{bmatrix} cos(th3) & 0 & sin(th3) & L1 * cos(th3) \\ sin(th3) & 0 & -cos(th3) & L1 * sin(th3) \\ 0 & 1 & 0 & 0 \\ 0 & 0 & 0 & 1 \end{bmatrix} \quad Eq\ 7$$

$$A4 = T_4^3 = \begin{bmatrix} cos(th4) & -sin(th4) & 0 & L2 * cos(th4) \\ sin(th4) & cos(th4) & 0 & L2 * sin(th4) \\ 0 & 0 & 1 & 0 \\ 0 & 0 & 0 & 1 \end{bmatrix} \quad Eq\ 8$$

$$A5 = T_5^4 = \begin{bmatrix} cos(th5) & -sin(th5) & 0 & L3 * cos(th5) \\ sin(th5) & cos(th5) & 0 & L3 * sin(th5) \\ 0 & 0 & 1 & 0 \\ 0 & 0 & 0 & 1 \end{bmatrix} \quad Eq\ 9$$

Forward kinematics is given by multiply all the transform matrixes (Eq 5, 6, 7, 8, and 9) together, which represent a homogenous matrix as shown in Eq 10

$$T_5^0 = T_1^0 . T_2^1 . T_3^2 . T_4^3 . T_5^4 = \begin{bmatrix} \mu_x & O_x & \alpha_x & p_x \\ \mu_y & O_y & \alpha_y & p_y \\ \mu_z & O_z & \alpha_z & p_z \\ 0 & 0 & 0 & 1 \end{bmatrix} \quad Eq\ 10$$

3.2.3. Thumb finger Kinematics modelling

Similarly, the forward kinematics configuration model for the thumb was obtained. From
The following Table 4 below shows the derived DH parameters for the thumb by utilising the same index method.

Table 4: DH parameters for the Thumb finger

i	θ_{i-1}	d_{i-1}	a_i	α_i
1	θ_1	0	$L0$	0
2	θ_2	0	0	90°
3	θ_3	0	L1	0
4	θ_4	0	L2	0

These parameters allow for obtaining the forward kinematics model.

$$A1 = T_1^0 = \begin{bmatrix} cos\ (th1) & -sin\ (th1) & 0 & L0 * cos(th1) \\ sin\ (th1) & cos\ (th1) & 0 & L0 * sin(th1) \\ 0 & 0 & 1 & 0 \\ 0 & 0 & 0 & 1 \end{bmatrix} \quad Eq\ 11$$

$$A2 = T_2^1 = \begin{bmatrix} cos\ (th2) & 0 & sin\ (th2) & 0 \\ sin\ (th2) & 0 & -cos\ (th2) & 0 \\ 0 & 1 & 0 & 0 \\ 0 & 0 & 0 & 1 \end{bmatrix} \quad Eq\ 12$$

$$A3 = T_3^2 = \begin{bmatrix} cos\ (th3) & -sin\ (th3) & 0 & L1 * cos(th3) \\ sin\ (th3) & cos\ (th3) & 0 & L1 * sin(th3) \\ 0 & 1 & 0 & 0 \\ 0 & 0 & 0 & 1 \end{bmatrix} \quad Eq\ 13$$

$$A4 = T_4^3 = \begin{bmatrix} cos\ (th4) & -sin\ (th4) & 0 & L2 * cos(th4) \\ sin\ (th4) & cos\ (th4) & 0 & L2 * sin(th4) \\ 0 & 0 & 1 & 0 \\ 0 & 0 & 0 & 1 \end{bmatrix} \quad Eq\ 14$$

Forward kinematics of the thumb is given by multiply all the transform matrixes (Eq 11,12, 13, and 14) together, which represent homogenous matrix as shown in Eq 15

$$T_4^0 = T_1^0.T_2^1.T_3^2.T_4^3 = \begin{bmatrix} \mu_x & O_x & \alpha_x & p_x \\ \mu_y & O_y & \alpha_y & p_y \\ \mu_z & O_z & \alpha_z & p_z \\ 0 & 0 & 0 & 1 \end{bmatrix} \quad \textit{Eq 15}$$

3.3. Simulation Results and Evaluation

In order to validate the developed index and thumb kinematic models, a simulation of their performance was run using the forward kinematics model. The model was initially in a flexed position, as described by q0, and then moved through the simulation to reach the ultimate standard (finger flexing) position q5. Various simulations were used to track the number of alternative final positions in order to study the system's overall behaviour and the model's performance. In this case, controlling alternative hand openings to grab different-sized objects may be understood as a measure to control alternate hand openings.

Figure 6 illustrate that Several point-to-point motions for the index finger were noted to be possible based on the findings of the simulation tests, starting at the initial position and ending at the final reference position. These movements are a decent approximation of a general finger relaxation movement (case 4), where the initially flexed position gradually transitions to a straightened state (case 1). Similarly, Figure 7 illustrate the simulation result of the 3D kinematic model with 4 cases to represent the thumb F/E approximation model

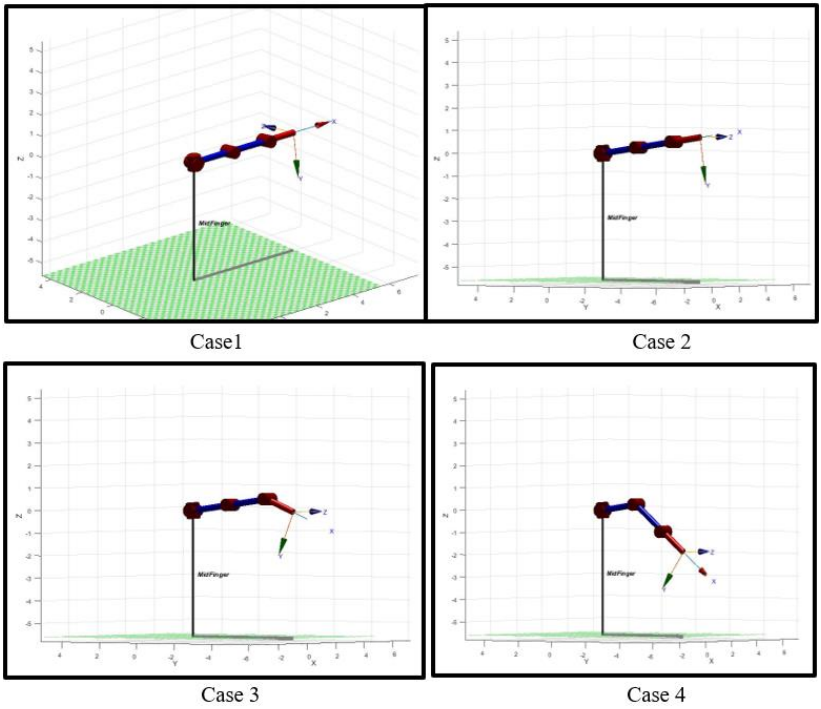

Figure 6: Simulation results for index finger.

case1, where, q1=0, q2=0, q3=0 , q4=0,q5=0. Case2, where q1=0, q2=90, q3=0, q4=0, q5=0. Case3, where q1=0, q2=0, q3=0, q4=0, q5=30. Where case 3, q1=0, q2=90, q3=0, q4=45, q5=0.

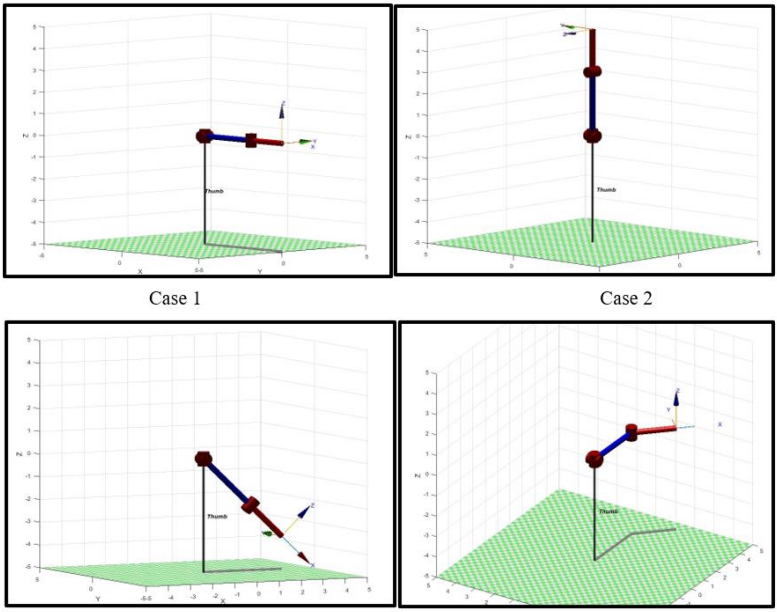

Figure 7: Simulation results for thumb finger.

case1, where q1=0, q2=0, q3=0, q4=0. Case2, where q1=0, q2=90, q3=0 , q4=0. Case3, where q1=0, q2=0, q3=45 , q4=0. Where case 3, q1=0, q2=0, q3=0 , q4=-45.

3.3.1. *2D Index finger workspace modelling*

Figure 8, exhibits a two-dimensional graph of one finger illustrating the workspace and simulated finger AROM. This is significant since it allows to visually finger F/E and draw the finger trajectory, which can then be compared to the physical measurement trajectories.

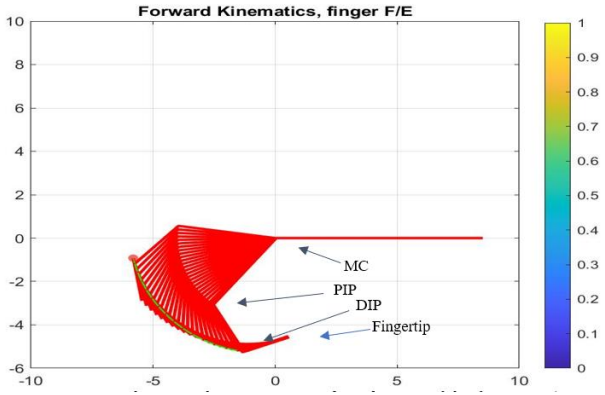

Figure 8: theoretical trajectories and workspace of the finger's F/E

3.3.2. Finger's Trajectory Planner Mechanism

To perform fingers F/E, 12 DOF must be actuated, divided into three for each finger joint (MCP, PIP, and DIP joints) To actuate all these joints obviously the number of the needed actuators and power will increase. This leads to an increase in the overall complexity, cost, weight, size, of the system as well as the machines that interact with the joints. The exoskeleton fingertip is designed to convert the driven displacement again into rotary motion, which is copying the finger's nature trajectory workspace.

3.4. Initial Design and Development

The initial finger's rehabilitation mechanism design (Figure 9) has the following characteristics: an indirect feed drives with a leading screw and a nut mechanism. The motor's torque operates a rotational angular velocity, which generates a dynamic force between the external thread of the leading screw and the nut's internal thread. In this design, the nut is positioned then fixed at the button of the worktable. The driven nut then induces a linear displacement to the work table. Eventually, this mechanism makes the rotational torque convert into translational velocity.

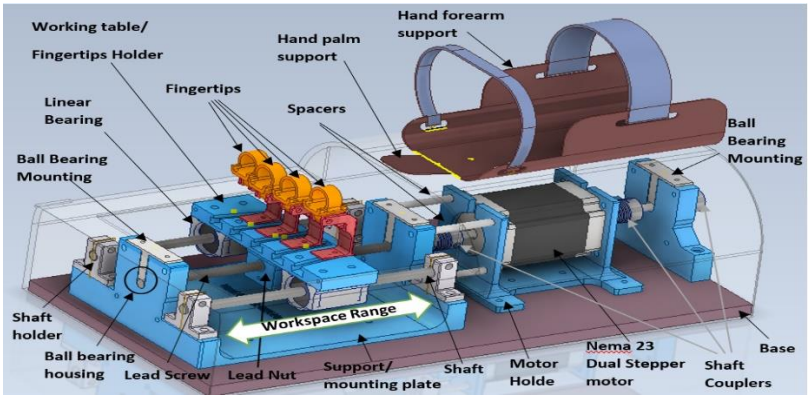

(a)

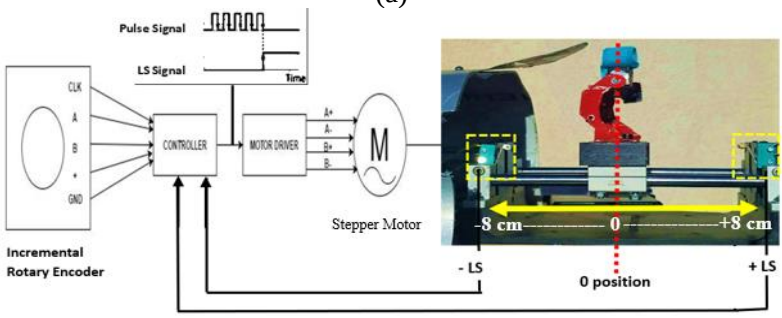

(b)

Figure 9: The grounded exoskeleton of the finger's rehabilitation mechanism design: (a), The Finger rehabilitation indirect feed drive screw and nut mechanism design with all parts; (b) Block diagram of the actuation system workflow

Exoskeleton fingertips were placed and fixed on the top of the worktable, designed to be the exoskeleton fingertip holder. The advantage of this simple mechanism is that the patient places their hand (load) onto the machine, leading to fewer mechanical parts integrations. This is considered a safety and comfort feature, not the opposite, where the mechanical assemblies are placed on the patient's fingers and top palm. Exoskeleton intestines are designed to be removable, changeable, and more hygienic.

However, it is crucial to define a starting position, which considers as a safety position. Therefore, before and after any therapy session, the exoskeleton fingertips return to their starting position (zero position). Figure 10 (b) demonstrates the summarized block diagram of the control working flow. The

actuator starts spinning until it reaches the worktable's maximum workspace physically clicks the first limit (+LS) switch. Once the +LS signals are registered, the controller disables the motor's driver's pulse signal. Eventually, that leads to stop the stepper motor, then return to the motor start spinning again in the opposite direction till the worktable reaches the other limit switch (-LS); once the -LS signal is confirmed, the motor driver provides the stepper motor with the required pules till it reaches the predefined zero-position.
After multiple experimental tests, the proposed mechanism was validated and the results indicate the ability of the proposed initial mechanism to smoothly guide the fingers in the opening and closing phases, it followed the desired trajectories with sufficient ROM as can be seen in Figure 18(a,b,c,d)

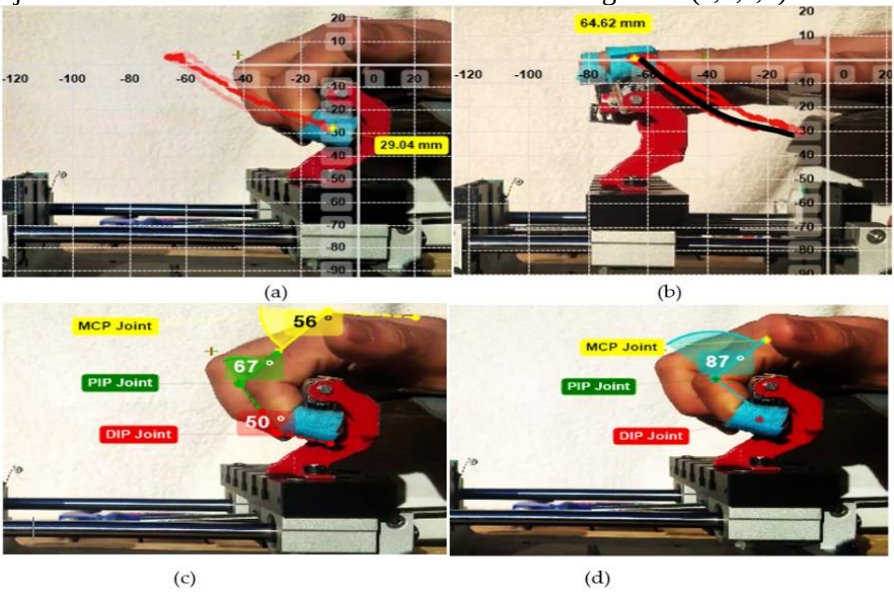

Figure 10: A real-time experimental setup of the index finger's workspace trajectories measurement: (a) Index finger fixation actual range of motion (ROM) angle, workspace trajectory, and position caused by the system. (b) index finger extension actual (black curve) and desired (black curve) workspace trajectory. (c) Index finger joints (MCP, PIP, and DIP) grasping ROM. (d) the overall grasping angle of the index finger.

Although the initial system could provide a sufficient ROM and trajectory guidance to four fingers, it could not provide a full extending range. Moreover, all the fingers had to move together, not individually, which made the design

not compactable for spastic patients. Additionally, the indirect leading screw mechanism generates a high vibration which could influence the therapy. Therefore, a major improvement needed to be taken.

Chapter 4: Ultimate System and Mechanism Design

Summary

- This dissertation presented a novel solution for four-fingers robot-base rehabilitation design and construction, providing repetitive, active, passive, and continuous passive training. We adopt a hybrid combination of ground-exoskeleton and end-effector mechanism. Additionally, this thesis developed a forward kinematics model representation for the dynamic part of the proposed mechanism it was mathematically represented to plot the predicted graphs of the robot's end-effector trajectories, positions, and velocity
- This dissertation developed embedded hardware (motherboard) with power management development to supply a stable voltage and sufficient required current for different electronic components that required a different voltage level. which consists of the essential parts such as, microprocessor, power management units, relay switching unit, cooling unit, motor driving unit, ADCs unit, signal conditioning filtering, amplification. Biofeedback sensory unit.
- This dissertation established a new embedded software (dashboard) and state management system. Python and JavaScript, alongside HTML and CSS, is mainly used for creating embedded dashboard and it back and frontend logics, and Vue.js. With the help of Socket.io and API programming languages were employed to make the hardware-software and software-software interfaces. Besides, a document-oriented

NoSQL database (MongoDB) was created to create a secured database system. In the backend development, a Hybrid control strategy of Impedance-Admittance controls the proposed active, passive and CPM therapy control modes throughout the developed embedded dashboard. Besides, an AAN controller was developed to provide the assistant as needed to end-users in their active training sessions.

- This dissertation presented a novel solution for the Thumb rehabilitation mechanism using only one actuator. The entire thumb mechanism was built to be adjustable so it can hold different hand sizes and shapes. Moreover, it meets with the thumb with only one MC. The whole mechanism is away from the dorsal side of the hand palm. This help to avert any conflicts between the mechanism and the hand. The thumb experimental results reveal its functionality to be effective in freely move the thumb without any irritation

4.1. Four Fingers Design Description

Based on the strike clinical and technical requirements coupled with the proposed system objectives. The proposed system's structure parts were designed to provide active and passive motion to fulfil the demands of various rehabilitation stages for both rights and left hand's fingers independently. The overall structure of the proposed system can be defined as a hybrid mixture of end-effector and grounded-exoskeleton mechatronics systems.
This section illustrates the various design characteristics of a novel four-fingers rehabilitation mechanism, including the whole structure of the proposed solution, Transmission and Driving mechanism, Exoskeleton fingertip mechanism design, and finger-robot integration.

4.1.1. Transmission and Driving mechanism design

Figure 11 demonstrates the proposed driving and transmissions mechanism is composed of a Servomotor and its holder, rack, pinion, and supporting rack home, supporting linear bearing and guiding shaft. The servomotor is fixed at the motor holder then directly mounted with the pinion. A spline, small grooves

along the shaft, and screw holes for firmly mounting servo horns make up the output shaft of the used servomotors. The rack is securely mounted into a rigid body at a fixed axis. When the rack is driven linearly, the pinion will be forced into the rotation if the rack moves linearly. In this mechanism, as soon as the motor's torque operates a rotational angular velocity, it generates a dynamic force between the teeth of the pinion and the rack. This leads to moving the rack at a fixed axis with predetermined displacement at either the forward or backward direction.

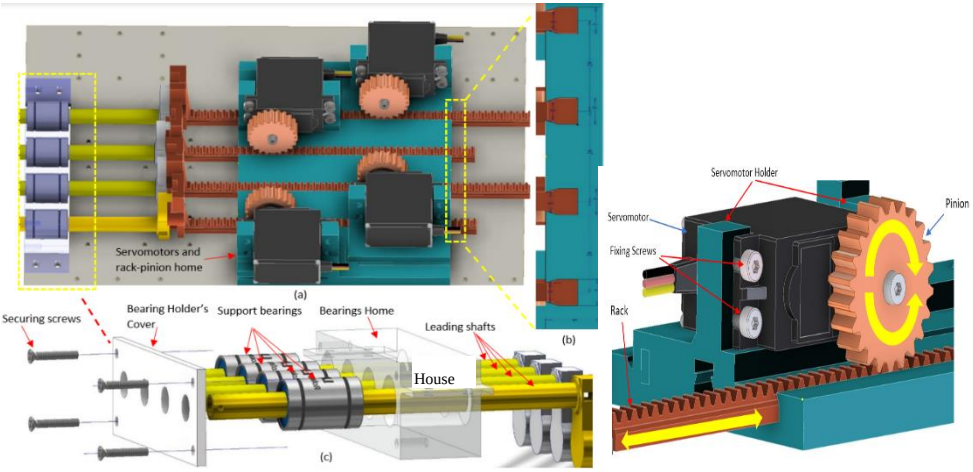

Figure 11: Ultimate 3D design of four-driving mechanism assembly: (a) the total driving and transmission mechanism; (c) back view of the rack housing; (b) supporting linear guide assembly

Figure 11 (a) shows the 3D design of the ultimate driving and transmission mechanism unit, which is structured to be driven by four servomotors. The same previously explained rack and pinion mechanism were employed to convert the rotary motion to a linear displacement. Figure 11 (b) present the dimensions of the custom-designed rack and the distance between each rack's centre, and another, 24mm, 7mm, and the rack's teeth 5mm; this customize rack was designed to be fit and secured into the rigid transmission and actuation unit.

4.2. Thumb Rehabilitation Mechanism Design

Thumbs are a critical element of human hands as they facilitate dexterity when humans grasp small objects. The thumb has a very complex structure and unique way of trajectory motion and ROM compared to other fingers. To perform

normal thumb F/E, the three joints of the thumb (IP, MCP and CMC joints) need to flex and extend within a certain angle as presented in Figure 26. In this section, we present and describe a novel solution design and mechanism targeting both rights and left thumbs. The proposed thumb rehabilitation design is not to perform such motion across the CMC joint.
It integrates with the thumb with only one MC at the thumb tip when the thumb is at around 60 degrees of its Radial Abduction position (Figure 26) This position helps to have smooth thumb F/E. Eventually, for prototyping purposes, most of the mechanical structure of the intended system was fabricated using a 3D printer (Prusa) and printed using PLA filaments.

4.2.1. Thumb rehabilitation mechanism Design process

Figure 12 shows a side view of the thumb rehabilitation prototype's 3D CAD assembly model. It mainly consists of a servo motor, motor holder, motion transmission mechanism, and thumb tip holder. The whole thumb rehabilitation design was secure and carefully mounted onto the same rigid aluminium base that used to hold the other four fingers entire mechanism from the other side. These help adjust mechanism length to match various hand sizes and naturally provide and/or follow the thumb motions.

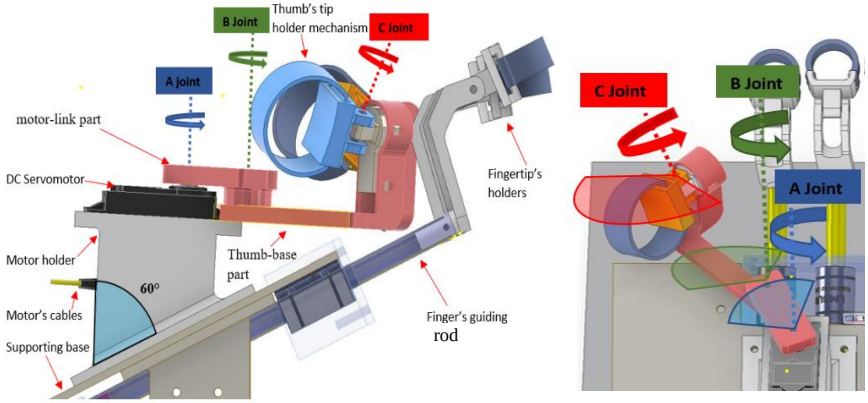

(a) (b)

Figure 12: 3D CAD structure model of the proposed thumb rehabilitation mechanism with its implementation. (a) side view. (b), top view, demonstrate the active ROM of the proposed thumb mechanism's links.

Figure 12 shows the possible workspace of each mechanical part with its joints of the proposed mechanism, starting from the motor-link part with its A joint. It is observable that the thumb holder at C joint is a little bit curved with a specific angle which is attentionally made to be more comfortable to the thumb tip. Through this structure, the entire mechanism will meet with the thumb with only one mechanical connection. This reduces the mechanical connections between the machine and the patients.
Eventually, Figure 13 demonstrates the proposed system with forearm cuff support and mechanism's cover and based.

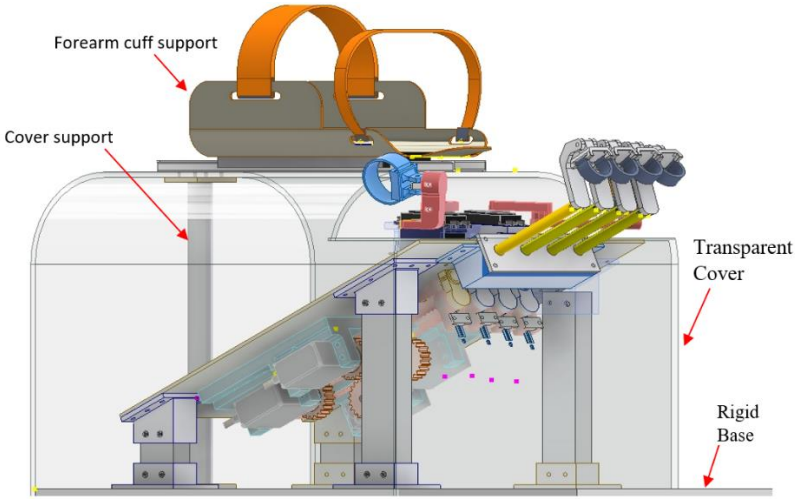

Figure 13: 3D structure of the proposed fingers rehabilitation system

4.3. Wrist and Forearm Mechanism Design

The wrist joint links the hand and the forearm together, the wrist formed by a series of eight carpal bones and a soft tissue wrapping them, basically the wrist important small joint anatomic planar structure. The wrist joint performs one DOF for wrist flexion/extension and one DOF for wrist radial/ulnar deviation [18], [19]. One DOF by the forearm joint process of supination/pronation (S/P), thanks to the elbow joint [20].
The proposed approach provides an active, passive and continuous passive motion to the wrist joint movement (F/E, R/U). The proposed system utilizes in total three servomotors to power these joint movements, as shown in Figure 14.

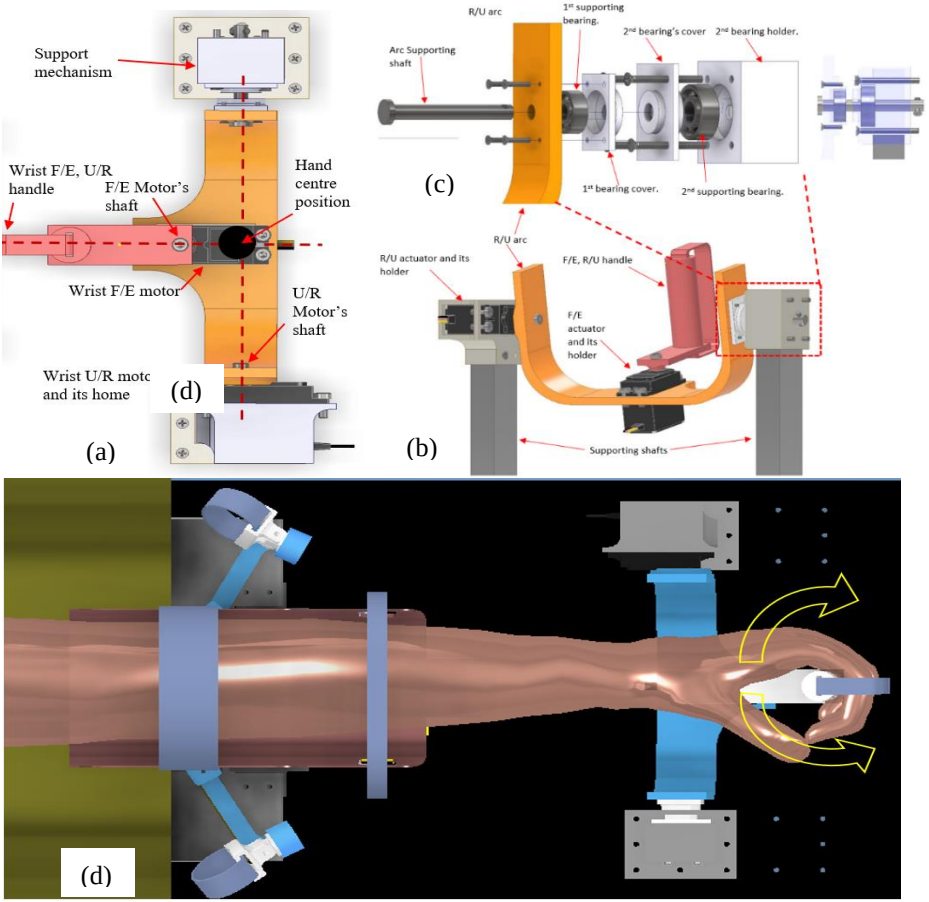

Figure 14: 3D structure of the proposed wrist and forearm rehabilitation system. (a), top view of the proposed wrist mechanism. (b) the entire structure; (c), arc supporting mechanism. (d), 3D model assembly of human-robot integration for the wrist

Moreover, the whole wrist and forearm proposed mechanism is connected into the same base of the fingers and thumb mechanism and it uses the same forearm support and control with the same controller and UI. This would keep the whole mechanism more compact and straightforward, and accessible.

4.4. Embedded Hardware and Software Development

The proposed comprehensive electrical and electronics system is shown in Figure 15. It consists of a microprocessor, power supply units, relay switching unit, cooling unit, motor driving unit, ADCs unit, and filtering unit. The AC/DC converter takes AC 110-260v as input, and gives 24 VDC, which is able of driving a 6A load with a high-efficiency current. This 6A is sufficient to power 5 servomotors running simultaneously in case of active fingers therapy. A second buck convertor, named MF-6402402, with adjustable output voltage, was employed to step down the 24VDC into 12 VDC. Both buck converters include built-in current limit features, which also include an internal MOSFET over the current protection mechanism.

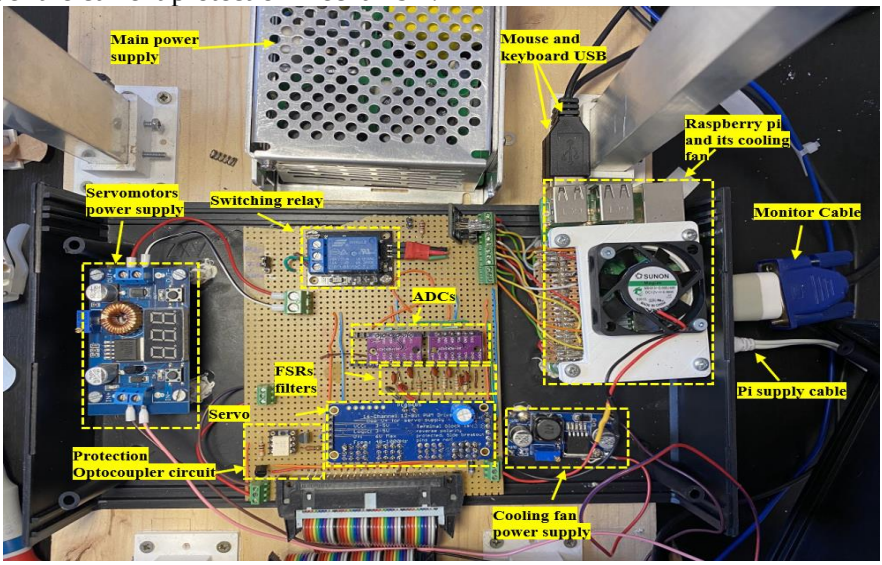

Figure 15: A low power consumption. illustrates the hardware composition and relationship.

4.5. Software: Back-End and Front-End Development

The Graphical User Interface (GUI) allows patients to interact with a developed user-friendly dashboard used in conjunction with the rehabilitation hardware and proposed control method. The specially developed UI was developed based on therapists suggestions; it provides an interactive and motivating training environment with feedback, based on measuring selected quantitative features of hand function such as ROM tracking and grabbing force. As can be seen in

Figure 16, the front-end of the developed UI consists of multiple tabs: patient information, session information, hand parameters, therapy, and evaluation. It simply works; when a patient comes, the therapist starts by writing the health insurance number of the patient or any ID number. Because this number is unique, the patient who is new or who came before can be checked easily by searching for the number in the database. If it is the patient's first time for therapy, fields can be filled, and a new patient file can be created by clicking the save button. And if the patient is someone who already came before. All his/her data can be loaded with the help of the load button. This data is store in a MongoDB database collection named patients. This tab contains data about both patient personal and stroke information.

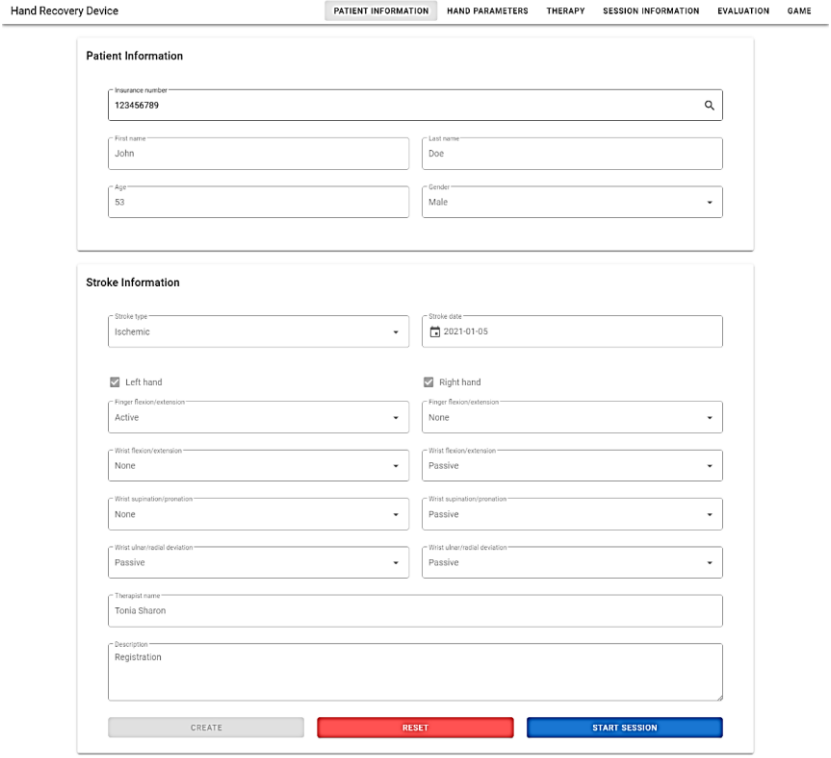

Figure 16: Front-end of a specially developed (Patient information tab on GUI)

One of the most used programming languages in the world is JavaScript. JavaScript is an implicitly typed language, which means the programmer does not need to define the type of variables. Interpreter manages the types for low-level languages [15]. JavaScript, alongside HTML and CSS, is mainly used for creating web applications. Many open-source JavaScript libraries/frameworks that help build web applications more accessible and Vue.js can be shown as an example. One of the benefits of this framework is the structure of the project. The structure of a page written in HTML, CSS, which is used to make the page look prettier, and the logic that determines how the page should react to different interactions written in JavaScript can be in the same file and makes component-based coding much more manageable. The variables that are used in components are reactive, which means when they have been modified the UI changes accordingly. With the help of a framework called Electron, websites can be converted into standalone desktop applications, and these applications are cross-platform, which means with one source code, the application can be used in different operating systems, such as Windows, Mac and Linux.

A. GUI and servo controller communication

Since servo motors do not support speed control by default. To achieve speed control, the angle of the servo motor can be changed gradually, which means, the angle will be incremented/decremented by step and there will be a delay in between steps. The speed control can be achieved by modifying steps and delays.

In Figure 19, the control method block is modular, which means it can be replaced with any controlling method. In Figure 17, the control method is replaced with Proportional Derivate (PD) controller and saturation block. Step and delay determine the speed of the servo motor. PD controller calculates the required step to reach the desired angle, but the output step can also be big, making the speed bigger. Because of security concerns, the step should be limited between maximum and minimum. That is why the saturation block is used. The servo motor is calculated and sent to the servo driver based on the limited step new angle of the servo motor. After sending, the application waits for a pre-defined time.

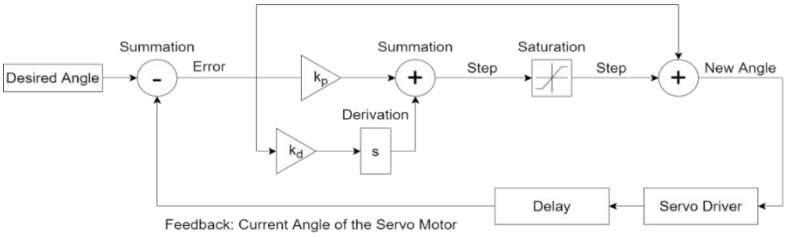

Figure 17: Servo motor speed and position control block diagram

The method for controlling servo motors and updating GUI based on sensor reading happens as below.

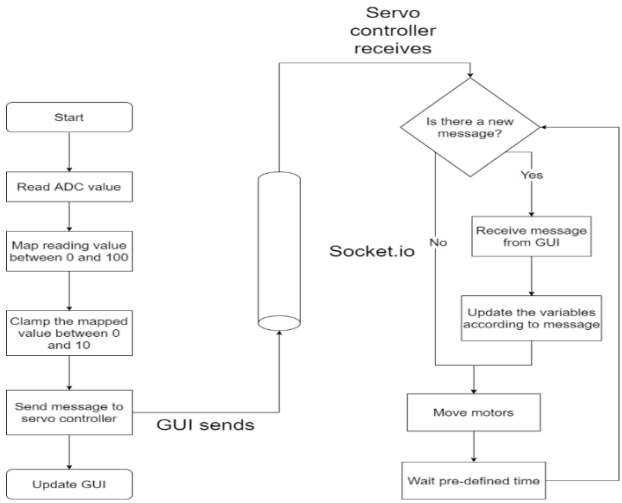

Figure 18: Controlling servo motors and updating GUI based on the sensor reading.

Thesis III: Related publications: [P1, P2, P3]

- **This thesis presented a novel solution for five-fingers robot-based rehabilitation. A forward kinematics model representation for the dynamic part of the proposed mechanism was mathematically**

represented to plot the predicted graphs of the robot's end-effector trajectories, positions, and velocity. A new implementation of developed control strategy of Impedance-Admittance controls, besides, an AAN controller provides active, passive and CPM therapy control modes. Eventually, quantitatively, and comparative studies supported by biofeedback (EMG) were achieved which indicated the efficiency and usability of the proposed system.

4.6. Forward Kinematic model of the proposed system.

A forward kinematic model was constructed and simulated for further investigations, mathematically represent the proposed system, and test and validate the kinematic behaviour of the proposed mechanical system. While the proposed robot with an end-effector may have several kinematic features indices, these are all connected to the robot's motions. For the finger rehabilitation process, the requisite coordinate systems must be constructed. The developed kinematic model with its reference frames is shown in Figure 19.

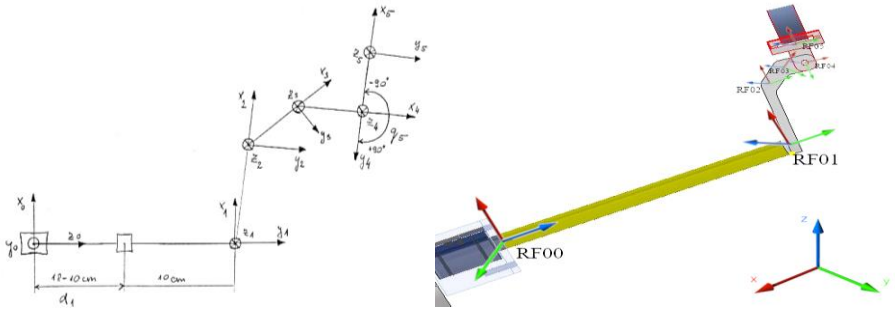

Figure 19: Coordinate frame of the proposed finger rehabilitation system. Detailed view of the robotic arm

For the sake of visibility and to keep the image legible, the axis names $(x_0, x_1, ..)$ were omitted. Instead, the Reference Frame (RF) was indicated, i.e., Reference Frame 02 is RF02 in the pictures. The Denavit–Hartenberg

parameters shown on Table 5 was defined considering the actual mechanical design of the driving and transmission mechanism with the end effector (fingertip holder).

Table 5: DH Parameters of the proposed system's end-effector

θ_i	a_i	d_i	α_i
0	0	100-180	90°
5°	30	0	0
30°	13	0	0
45°	10	0	0
θ_5	6	0	0

Workspace

All the values from the DH-table are defined as constant but two: d1 and Theta 5 since they will be the changing variables. Then, it is vital to notice that the transformation matrix for a prismatic joint is slightly different from a rotational joint.

$$T_{10} = \begin{pmatrix} cos\,(\theta_1) & -sin(\theta_1)cos\,(\alpha_1) & sin(\theta_1)sin\,(\alpha_1) & 0 \\ sin(\theta_1) & cos(\theta_1)cos(\alpha_1) & -cos(\theta_1)sin(\alpha_1) & 0 \\ 0 & sin\,(\alpha_1) & cos\,(\alpha_1) & d_1 \\ 0 & 0 & 0 & 1 \end{pmatrix} \quad Eq\ 16$$

$$T_{21} = \begin{pmatrix} cos\,(\theta_2) & -sin(\theta_2)cos\,(\alpha_2) & sin(\theta_2)sin\,(\alpha_2) & a_2cos(\theta_2) \\ sin(\theta_2) & cos(\theta_2)cos(\alpha_2) & -cos(\theta_2)sin(\alpha_2) & a_2sin(\theta_2) \\ 0 & sin\,(\alpha_2) & cos\,(\alpha_2) & d_2 \\ 0 & 0 & 0 & 1 \end{pmatrix} \quad Eq\ 17$$

For joints 3, 4 and 5 the matrix will be the same, just changing indices.

The final transformation matrix will be given by: T50 = T10 * T21 * T32 * T43 * T54;

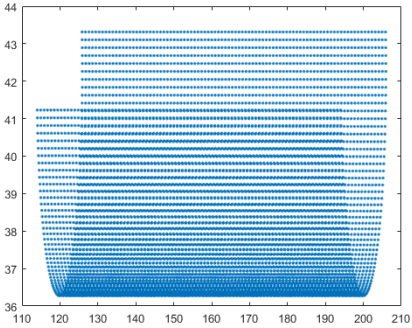

Figure 20: Robot's end-effector workspace plot

a) Trajectory

To build the robot model using Peter's Corke toolbox, the following links were created, respecting the DH-table.
L(1) = Link ([0 L1 0 pi/2 1],'standard'); %The "1" parameter indicates that this is a prismatic joint
Initial and final states should be defined as a vector with 5 dimensions, for prismatic joints the dimension will be the length, and for rotational joints will be the angle:
%This is the initial state for the robot, theta = 0, to visually verify how
%the robotic arm will stay at this orientation.
q0 = ([100 pi/32 pi/6 pi/4 -pi/2]);
%This is the final state, so the trajectory can be plotted.
qf = ([180 pi/32 pi/6 pi/4 pi/2]);
To plot the trajectory, the simulation considered the initial state as $\theta_5 = 0\,°$ and the final state as $\theta_5 = 180\,°$ and the prismatic joint varying from 180 to 100mm.
But, considering the Peter Corke Robotics Toolbox, the simulation will go from -90 to
90 (always in radians).
Figure 14, demonstrates the proposed system's end-effector while Figure 15,16 illustrates the modelling trajectory results, which show approximation results to the working trajectories and positions of the proposed system.

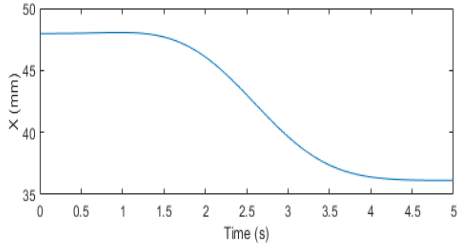

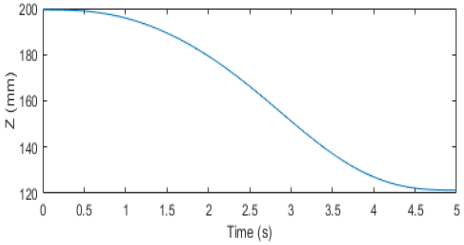

Figure 22: X and Z position for the end-effector (When the joint 5 goes from -90 to 90 degrees.)

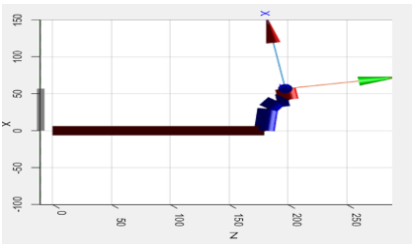

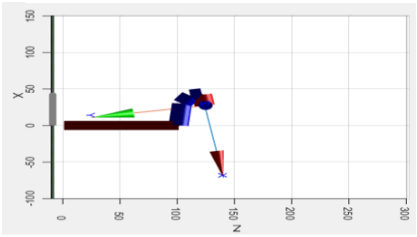

Figure 21: 3D Driving transmission mechanism of the proposed system end-effector: (a) Theta5 equals to -pi/2; (b) Theta5 equals to pi/2

4.7. Experimental Test and results

The quantitative and objective findings would help understand the proposed system openness. A timestamped evaluation of distinct motions that the patient makes across multiple sessions to evaluate the progress performance of the therapy sessions over time. Eventually, a subjective study was conducted based on the user's feedback to test the proposed system usability and comfortability. Figure 23, shows the human-robot integration

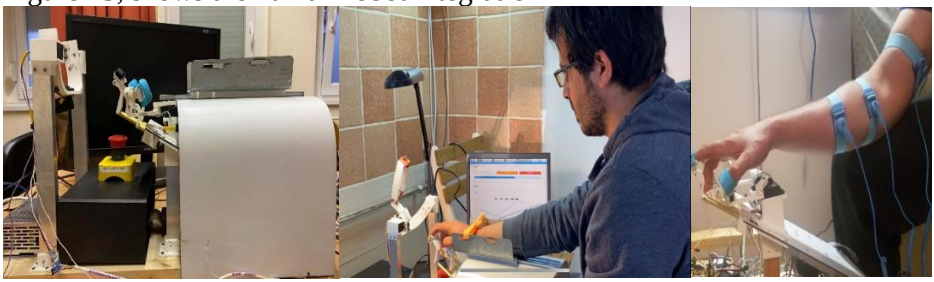

Figure 23:The proposed System implementation, human-robot integration setup

4.7.1. Passive Therapy: Experimental Test

After the participant's arm and fingers are properly fastened onto the fingertips holder using a Velcro strap. Passive therapy can be selected for the desired joints. From Figure 24 once, the session starts with measuring the hand parameters of the patient With the help of this tab, the maximum and minimum angles and displacements for movements are measured. For security, when measurement starts for any joint, everything on the UI is disabled except the one that has been started. This prevents starting multiple measurements by mistake and locks the GUI. As a result, other tabs cannot be selected. The proposed system allows the therapist to select the fingers extension and flexion ROM, to be generated towards each finger individually depend on the spasticity level of the patients, through the developed sliders. Each slider corresponds to a finger as can be seen in

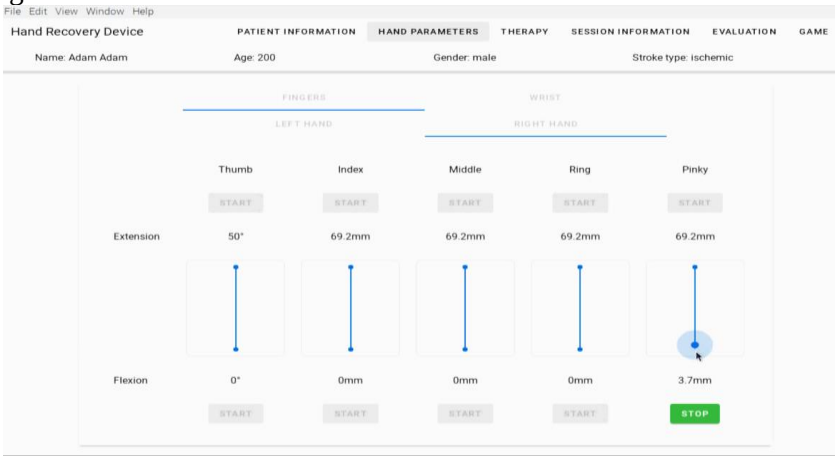

Figure 24: Hand parameters tab on UI

Through Figure 25, the first and end-users can observe a real-time graphing of the selected ROM, which encourages and psychological feedback to the patients about their abilities to perform active motion later. From the presented real-time graph data, it is observable that all fingers are moving independently from one other with different ranges of motions with low rpm; this result indicates the

ability of the proposed system to guide the attached fingers and move them smoothly and repeatably.

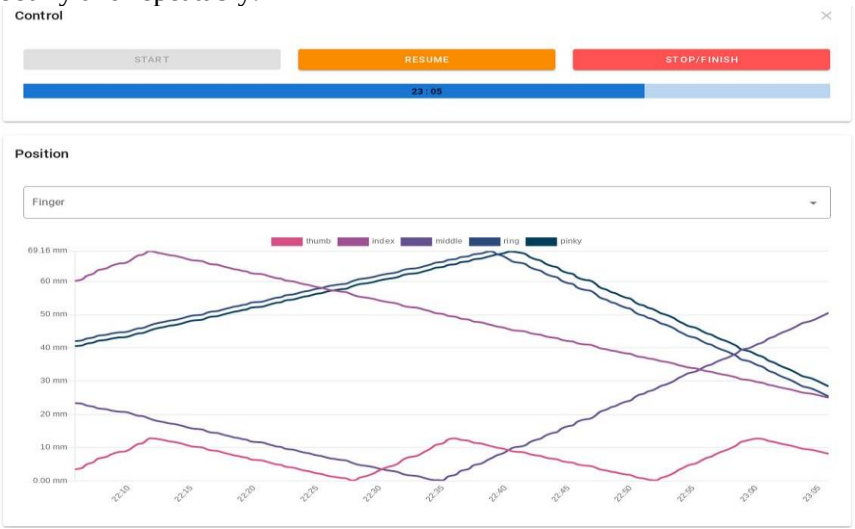

Figure 25: Real-time, passive finger F/E therapy training.

4.7.2. Passive Fingers F/E Experimental Results and Discussion

To collect more quantitative and objective results, a motion capture data acquisition system was set using Kinovea® software. To generate a comparative result of the trajectories and ROM acquired during freehand movements (without the proposed system) and sets them as desired trajectories and ROMs. On the other hand, the actual trajectories, positions, and ROMs are caused by the proposed system (with the proposed system). Figure 26 (a, b) elucidates the experimental implementation performing a continuous passive motion of the finger F/E. The solid red curve demonstrates the fingertip workspace trajectory caused by the proposed system, and the solid black curve again illustrates the fingertip trajectory workspace without the proposed system. In contrast, the yellow highlighted angles tracker presents the finger ROM of opening and closing the index finger in the set coordinate frame. It is easy to confirm that the actuated finger phalanx movement caused by the proposed system is within the natural functional trajectory workspace of the index finger phalanx. And both trajectories are closely associated with each other.

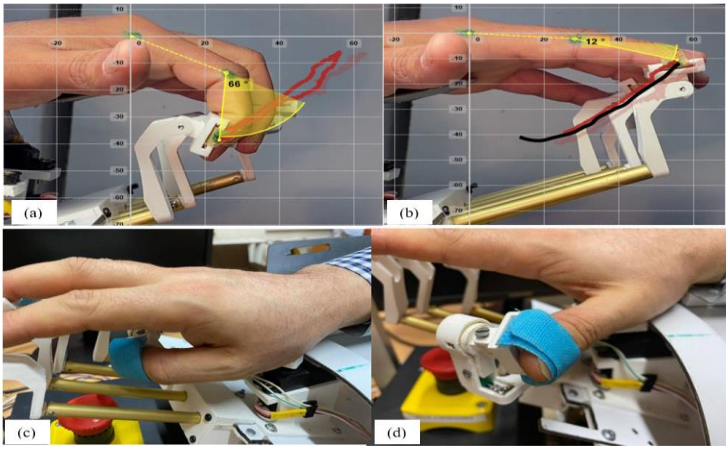

*Figure 26: A real-time experimental setup of fingers-robot integration and the index finger's workspace trajectories measurement:(**a**) Index finger extension actual ROM angle and workspace trajectory caused by the proposed system; these ranges are considered within the normal functional grasping range of motion of the index finger. (**b**) index finger flexion actual (red curve) and desired (black curve) workspace trajectory. (**c**) thumb finger flexion induced by the proposed thumb mechanism. (**d**) thumb finger extension induced by the proposed thumb mechanism*

Besides, graphical descriptions were accomplished by analyzing the video data used for both the index finger opening and closing phases. Figure 27(a, b) shows a comparative analysis between; (1) the desired fingertip displacement, which plotted a solid blue curve; (2) the actual fingertip displacement induced by the proposed system, which is plotted by solid orange. It is straightforward to understand that the participant performed a finger flexion and extension two times, and the plotted displacements are in both vertical and horizontal orientation, respectively. Figure 27 (a) plots the horizontal X-axis, while Figure 27 (b) describes the vertical displacement in the Y-axis.

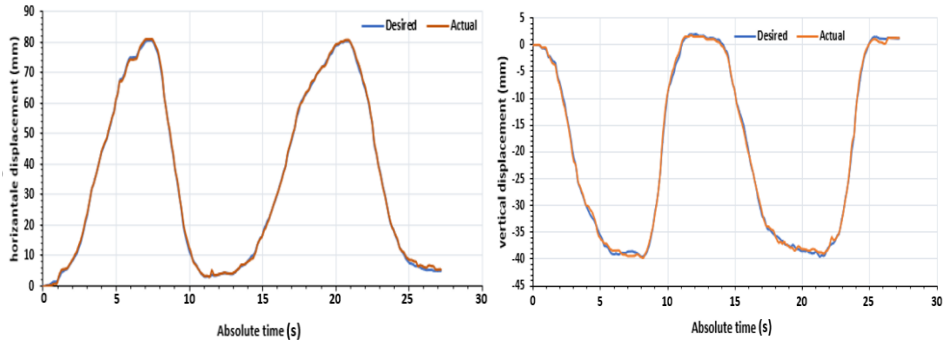

(a) (b)

Figure 27: Continuous passive motion rehabilitation experiment of s typical finger flexion and extension displacement. (a), the fingertip displacement in horizontal; (b), the fingertip displacement in the vertical axis.

Moreover, we can also observe that the proposed system drives 80 mm of total displacement at the horizontal axis to open and close the index finger and −39 mm displacement at the vertical axis; these displacements values are considered within the normal functional range of the index finger. Besides, the actual guided trajectory corresponds to the planned desired trajectory, and all the finger joints (DIP, PIP, and MCP) travelled concurrently without any movement discomfort. Accordingly, the results indicate that the motion of the finger rehabilitation design is stable. However, it can be observed that the actual and desired displacements of the DIP phalanx have a small percentage of error during the execution of the movement. It is worth noting an error percentage, about 0.874% error at the vertical axis and 1.257% error at the horizontal axis. The error rates are limited mainly by the friction between the external threads of the rack and the external threads of the pinion, and the vibration caused by the movement. However, these minor errors do not influence the continuous passive motion (CPM) rehabilitation characteristics and the proposed device's performance.

4.7.3. Active Therapy with Assistance

In the active therapy, the patient is supposed to have enough grabbing force to actively move their fingers or wrist; however, it is possible that they can move their fingers actively but do not have enough grabbing force to move the robot's end-effector. Therefore, the proposed system first measures the grasping force capabilities force, and once the patient applies a small amount f force within the 5N stress range, the proposed system will passively move the fingers whenever the patients apply an active force. With this in place, end-user with Neuroplasticity will be more motivated to perform out with the proposed system's support; the control logic behind this concept is known as the assist-as-needed (AAN) control strategy. By having the patient perform the movement themselves, they have to invest a considerable amount of effort. Hence the AAN technique prioritizes minimizing the use of robotic aid for this purpose. The proposed system motion's support is discontinued if somehow the user can do the required operation. The assistance is provided just as much as is necessary.

From the control dashboard, the active therapy can be selected; then, the patient is asked to apply an active force to move the guiding mechanism. Initially, the applied forces will be measured in real-time, and the motors will be moving within a limited range; that range will be selected depend on the patient case, which means the grasping force abilities and the AROM that patient can perform. Once these ranges have been registered and stored, the therapy can be started and limited to these ranges that have been predefined. This considers as a safety feature to product the patients with limited AROM due to spasticity.

Figure 28: The developed control dashboard: hand parameters selection

According to the experimental results, the system waits for the patient to apply an active force; when this state condition is approved, the fingertip holder starts to flex the finger with slow-motion till it reaches the maximum predetermined range, if the patient keeps applying force, the fingertips holder will maintain the maximum predetermined position, and once the patient released the applied force, the device will passively move the fingers to the predetermined extension position. Figure 29 indicates a real-time experiment in which the fingers perform an active therapy with assistance, Figure 29 (a), shows the performed ROM displacement in X-axis, for four fingers; it is observable that each finger performed three times finger F/E with different ROM. It can also indicate the muscle activation recorded throughout an EMG sensor to show the muscle activities while the participant performs an active therapy through the fingers

opening and closing, as shown in Figure 29 (b). In order to assess the signal detected from the bare hand when it is clutching the fingertips' holder, the EMG signal analysis is performed. While the ranges of the interaction force between the participants and the robot's fingertips holder are within the range 0- 5N, as demonstrated in Figure 29 (c). The middle finger applied the maximum interaction force, and that it is why it reaches the highest ROM, which can be explained that the middle finger is the bigger and stronger among the other fingers. Follows by the index, ring and pinkie fingers. From Figure 29 the red highlighted to represent the fingers flexion phase, in which the interaction force is applied, while the green highlighted represents the extending phase in the interaction forces released

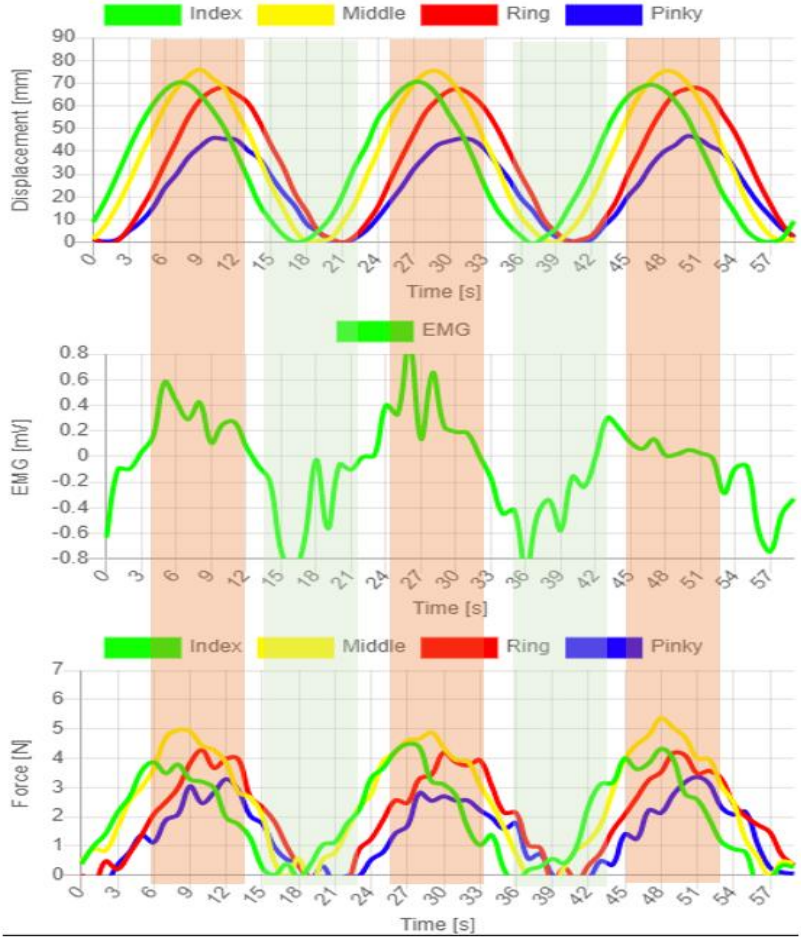

Figure 29: illustrates the real-time performance of active therapy with assistance. (a) four fingers ROM displacements. (b) shows the EMG signal analysis of a human during the active therapy with assistance with high muscular effort is during grasping periods. (c), the grasping force applied onto the fingertip's holder to perform active therapy.

Thesis IV Related publications: [P1]

- **This dissertation presents a novel approach and implementation of five Integrative tactile sensors that were developed and validated to drive a force-feedback to the developed AAN controller designed to assist the patients with their active therapy. Additionally, it is also utilized to measure and evaluate the fingers pinch-tip strength measurement. Moreover, the developed algorithm analyses the collected forces data stored in the developed document-oriented NoSQL database (MongoDB) for progression evaluation report and presented in real-time during the therapy through the embedded developed GUI dashboard. Besides, a biofeedback sensory was implemented and detect the muscle activities through EMG signals.**
- **This thesis developed a time-based performance self-assessment; this feature enables the therapist and patient to detailly investigate and observe the recovery progress of the fingers in terms of grabbing force and ROM, the developed algorithm works based on performed maximum flexion and extension. This feature is taking the related technologies a step farther to make them not just robots for training but also as evaluating instruments**

Chapter 5: Design And Development an Integrative Grabbing Force Sensing Unit

5.1. Overview

A piezoresistive sensor (FSR) sensors were embedded on the device to serve as a force sensor, and the grabbing force data will be collected and shown in real-time during the therapy through the developed GUI. The proposed design helps the therapist and the patient easily monitor the improvement process by monitoring the grabbing forces after each therapy session or group of sessions.

5.1.1. Design Of the Integrative Force Sensing and Working Principle

The modular grasping force sensing's entire mechanical structure is illustrated in Figure 30 (a, b) The proposed structure mainly consists of a sensor base, FSR sensor, sensor contacting cover, spring and rack-guiding shaft connection point. The sensor base follows the structure of the FSR sensor so part of the flexible substrate of the sensor is secured with a cover to avoid any vibration that can affect the sensitive area of the sensor. A solid round tactile pad was applied into the face FSR cover, with the portion of the force sensor that is sensitive to variations in sensitivity glued to the pad.

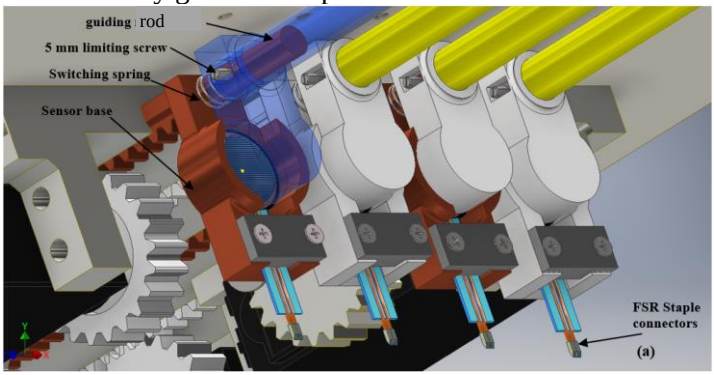

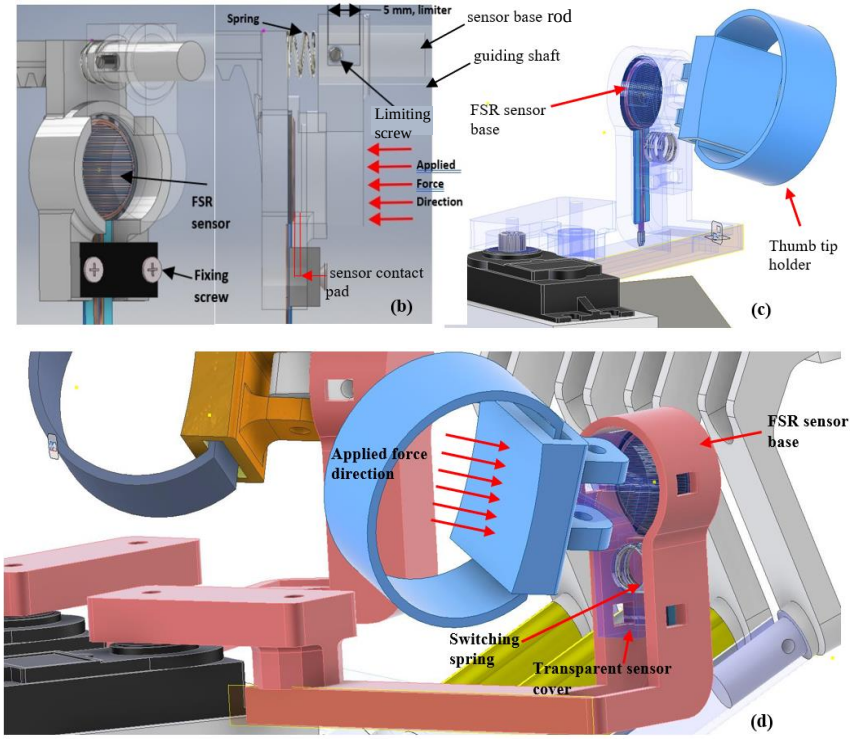

Figure 30: 3D structure of developed Integrative Force Sensing*:*

(a) 3D CAD structure of the proposed grabbing force mechanism which consists of four integrative force sensing units for four fingers. (b) The detailed structure of the FSR sensor module, in which the contact pad is used to improve the sensitivity and stability of the FSR sensor and switch spring to avoid undesired contacts. (c, d) the thumb tip proposed an integrative force-sensing measurement approach. Which mainly consists of, FSR sensor, Sensor base, sensor cover with contact pad, and switching spring.

A mechanical spring is added to the design to prevent constant contact between the sensor cover pad and the sensitive area of the sensor base. The advantage of adding the sensor it makes the whole integrative force sensing mechanism like a normally open switch. When the patient applies a small amount of force on the fingertip holder that force will be transmitted to the sensor, forcing the spring to be compressed and make contact over the sensor within a 5mm limited linear distance.

5.2. Electromechanical Implementation

In this section, the physical implementation of the structure of the proposed design. Figure 31 (a) demonstrates the physical integration of the proposed design main complement, including the FSR sensor, guiding shaft, sensor cover, and sensor base. Figure 31 (b, c) illustrate the working principle of the proposed design,

1. Figure 31 (b) shows an external force acting on the fingertip holder that transferred to the sensor cover. This force makes contact between the sensor sensitive area and sensor cover contact surface; it is observable that the spring was compressed because of the applied force.
2. While in Figure 31 (c), shows when the force was released from the fingertip holder, which is the natural state. In this case, the spring-applied force in the opposite direction releases the contact between the FSR sensor sensitive area and the senor cover connected surface.

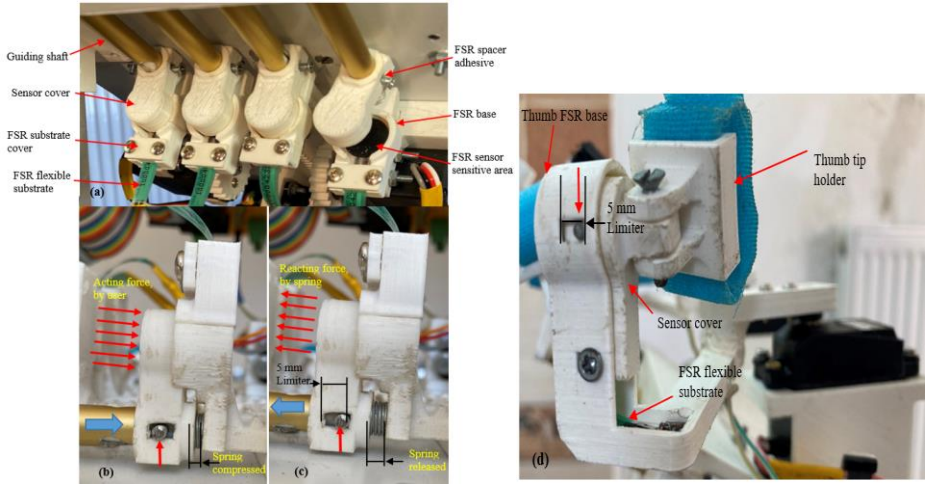

Figure 31: Electromechanical Implementation.

(a), physical integration of proposed integrative design main complement. (b, c) the two cases when there is, and there is not grabbing force applied onto the sensor sensitive area.

While Figure 31 (d), illustrates the thumb rehabilitation mechanism and the force-sensing design; the thumb integrative force sense follows the same described working principle. However, the whole mechanism of the four fingers and two thumbs (right, and left) was tested and showed promising results.

However, to get the best readings, calibration and signal conditioning, including filtering and amplifying the FSR readings were needed.
For the measurements, the sensor's resistance varies between 3kOhm and 30kOhm when activated; the pressure range is from 0.5N/cm2 to 100N/cm2. Since raspberry pi does not support analogue input, an ADC should be used, in this case, it is MCP3424. This ADC has 4 channels and 4 different resolutions (12, 14, 16, and 18 bit) [16]. ADC and raspberry pi communicate using the I2C protocol, and one of 4 different addresses can be assigned to the ADC by setting address pins to high or low [16] . The converted reading of the sensor is between 0 and 2.048. Because this range does not make much sense, the range can be changed with the help of the range function as below. After mapping, the range will be between 0 and 100 which is the force that can be measured by the sensor.

$$M = (X - I_{\min}) \times \frac{(O_{max} - O_{\min})}{(I_{max} - I_{min})} + O_{min} \qquad (7.)$$

X – Reading of the ADC
I_{max}, I_{min} – maximum and minimum output of the ADC
O_{max}, O_{min} – resulting range
Since 100N is such a big force and it is not usual to see that much force being exerted by a finger, the mapped reading should be clamped in between more realistic values, which is in this case, between 0 and 10.

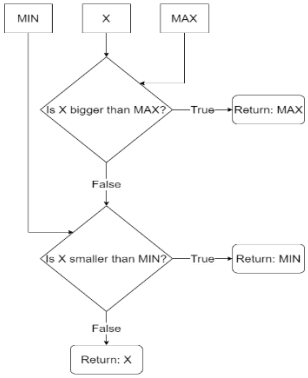

Figure 32: Clamping function

There are two ways of reading the sensor data. The first is the UI requests new data when it is required. The second is the UI requests for starting a stream, and

the ADC controller sends the new data in real-time until the UI does not need it anymore.

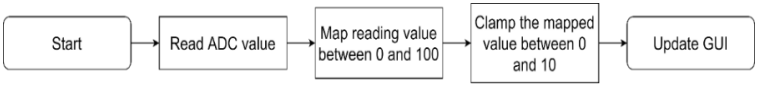

Figure 33: Updating GUI based on the sensor reading.

5.3. The Force Measurement and Evaluation

in addition to delivering the force-feedback, the proposed system was also constructed to aid the patients in their self-managed rehabilitation exercises. This increase the usability of the proposed system to help self-managed rehabilitation exercises be as simple and cost-effective as possible. in order to determine how much grabbing force the patients were capable of applying, a force measurement diagnostic feature was designed. Though this was conceivable, it was also conceivable to create an instrument to evaluate tip-pinch power, which is a component of hand functions examined on stroke patients regularly to evaluate their functional results [17]. Owning FSR sensors in the proposed system, it was also programmed to be used for the.Figure 34 present the developed force integration UI and the results of the five fingers. Moreover, this system can be used for either the right and left hand's fingers.

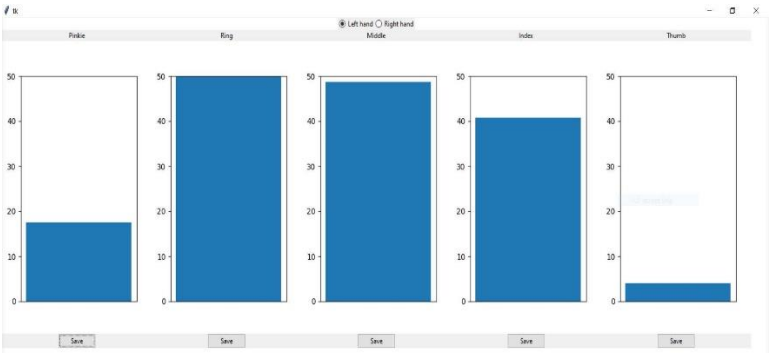

Figure 34: the developed force integration UI of fingertip-pinch force evaluator

5.4. Time-based Performance Assessment

At the end of each therapy session, the therapist and patient can detailly investigate and observe the recovery progress of the fingers and the wrist, based on performed maximum flexion and extension. From the developed dashboard and after hand parameters measurement and therapy, the session can be saved. It requires the date of the session, and optionally description can be added, as can be seen from Figure 35.

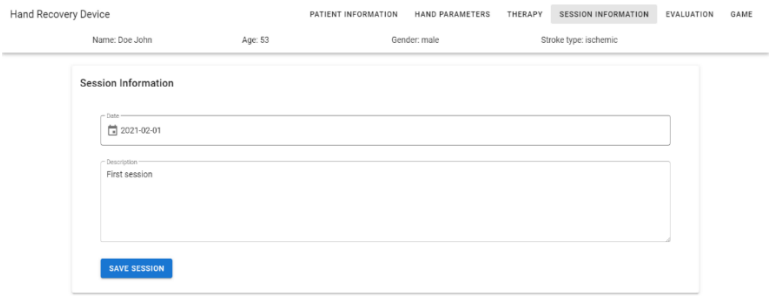

Figure 35: Session's information tab on the developed dashboard

At the end of each therapy, the therapist can store the preform sessions' parameters such as the maximum ROM, displacement, and interaction force. Additionally, after each session, the therapist can monitor these parameters progression that the end-user could perform throughout the session by accessing the time-based report assessment. To evaluate this feature of the proposed system. Figure 36 demonstrates the patient's time-based self-ROM assessment of various motions done over various sessions with varying dates and times. Figure 37, demonstrates the evaluation graph and report after 11 days of sessions, the progression graph Side and movement options change based on the data selected in the patient information tab. If different options are selected, the graph will be updated according to the chosen options. The graph will be saved when the save button is clicked. The x-axis in the example graph indicates the date, while the y-axis in the case of the index, ring, middle, and pinkie shows the displacement value, and the y-axis in the case of the thumb indicates the ROM angle. Besides the data graph presentation, each therapy's comments can also be shown in the description. This gives the proposed system the feature of friendly use by saving and reminding the therapist by its own comments, which can be used to describe the patient or the session status at the therapy time. It

appears that assessments demonstrate considerable improvement in performance before and after training.

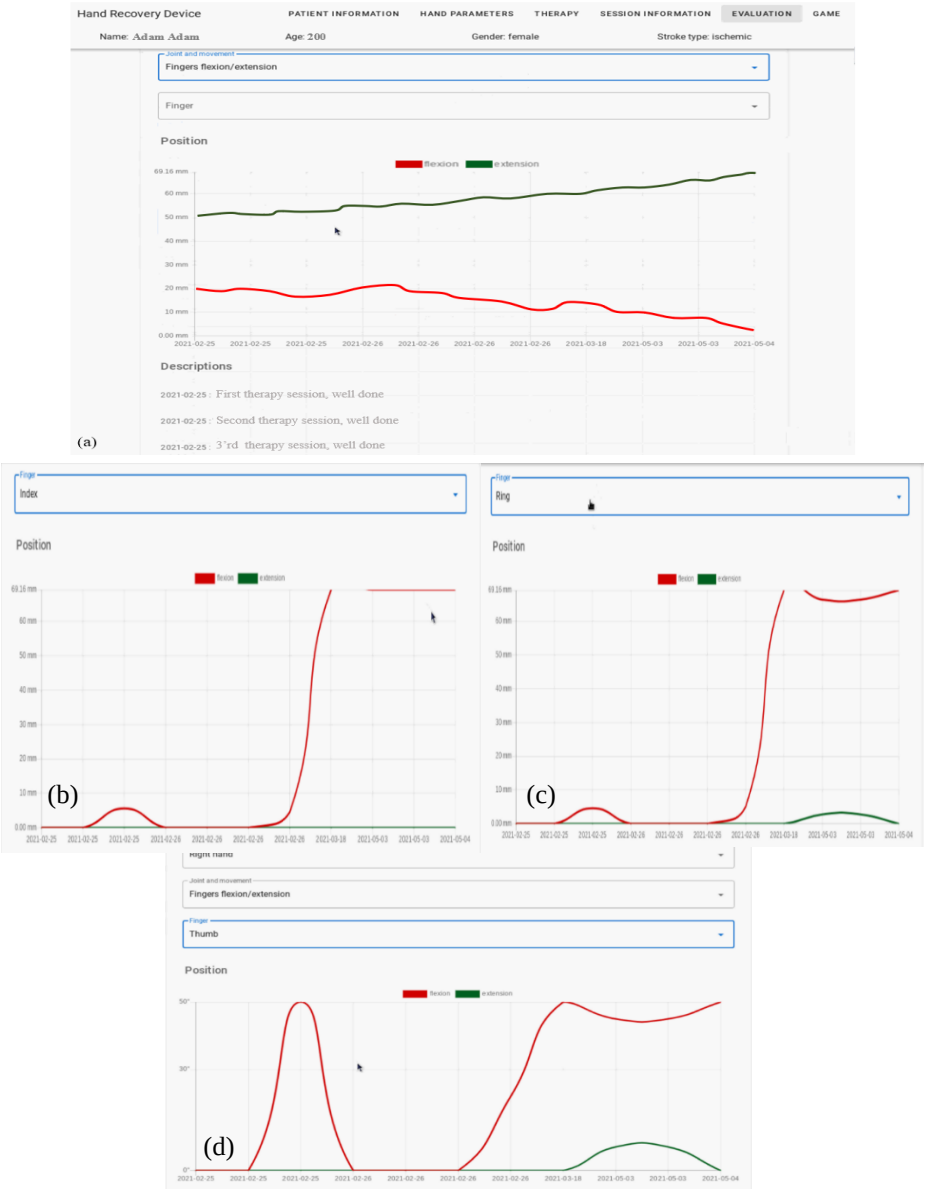

Figure 37: Time-based monitoring of the performance assessment. (a), time-based monitoring of the performance assessment after 11 sessions. (b), time-based index finger F/E assessment. (c), time-based ring finger F/E assessment. (d), time-based thumb finger F/E assessment

Thesis V Related publications: [P1, P3]

- **This thesis presents a new robot-based wrist rehabilitation system development that provided active, passive, interactive mode therapy for the wrist F/E and R/U. The proposed development was tested with a repeatable experimental test; the results are sufficiently accurate in aspects of the stability and trajectory's alignment; the actual trajectory directly correlates to the desired trajectory, which meets the requirements of continuous passive motion training configurations. In active training mode, the proposed system could guide the participant to perform wrist F/E and R/U; additionally, uniaxial and elliptical boundary motions could be performed, which increase the participant ROM and trajectory's workspace**
- **This dissertation has presented the development and evaluation of new interactive game-based rehabilitation, which provided an engaging and amusing experience for individuals with wrist impaired motor capability; the game-based therapy guides the users to perform multiple wrist F/E and R/U deviation gestures with random directions. The archived scores were stored and evaluate the participant performance.**

Chapter 6: Active and passive and interactive-based wrist rehabilitation system development

6.1. Wrist F/E and R/U Mechanism

The proposed mechanism actuates each joint with a single actuator but with one handle. This means the end-user needs to have the grabbing capabilities to hold the handle through the therapy sessions. The wrist F/E actuator is mounted in the middle of the arc, the F/U actuator's output shaft is connected to the handle mechanism. Perpendently, form the other edge side of an arc is connected into an arc supporting mechanism through an arc supporting shaft. Eventually, the whole wrist R/U rehabilitation mechanism was supported and fixed from each side with an aluminium support shaft.

6.2. Wrist Rehabilitation Experimental Results

Similar to the previous method of the finger's F/E, the initial setup was applied in the case of wrist F/E, and R/U. The proposed wrist rehabilitation system adopt passive, active and interactive control mode therapies. To be able to compare the nature wrist motion (without any passive assistance) with the wrist motion that guiding or induced by the proposed system. The nature wrist motions were studied and analyzed with and without the proposed device, then later it will be compared with wrist motion caused by the proposed. In this experiment, we selected the desired ROM for wrist F/E to be (0°–45°/0°–25°); these degrees were chosen to be within the wrist's normal. Using the motion capture system, passive markers and angle measurement markers were located on the targeted joint to acquire these ROM angles and trajectories; After the therapy started, the system moved smoothly according to the preselected ROM with low rpm. As shown in Figure 38 (a), the end-user started forming the nature position (0°) then performed flexion and wrist extension gestures.

Additionally, from Figure 38 (a, b, c), we can see; (1) the desired workspace trajectories of the wrist F/E demonstrate black curve demonstrates the workspace trajectories (without the proposed system); (2) the actual motion of the wrist F/E workspace trajectories (with the proposed system) which indicated by the blue curve. In regards, the yellow highlighted value presents the current position of the wrist in the predefined coordinate frame. Besides, it can also be observed that the two trajectories are relatively identical towards one another, and the participant has confirmed that there is no movement discomfort of the device. Eventually, the actual (with proposed system) ROMs of the wrist F/E are (0°–44°/0°–25°).

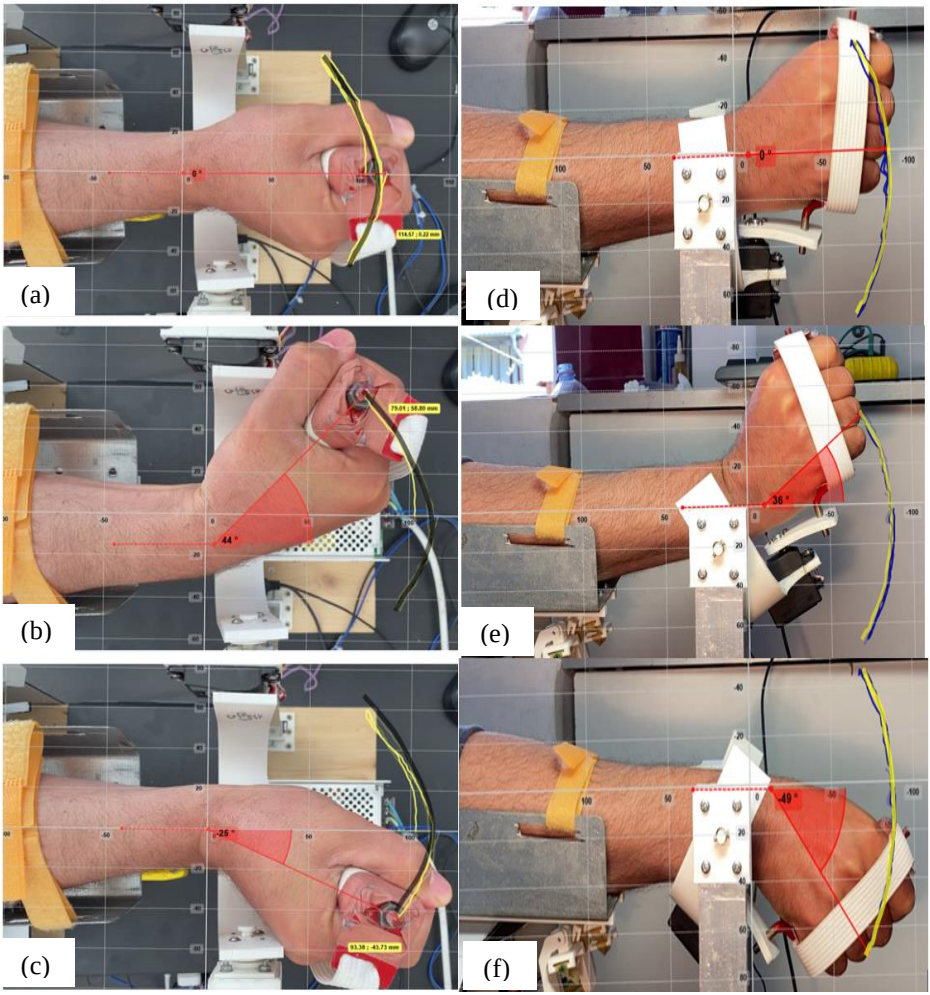

Figure 38: The real-time experiments of wrist F/E and R/U workspace trajectories and ROM. (a), the comfortable wrist position (zero position). (b) actual wrist flexing (yellow curve) and desired (black curve) workspace trajectory, position, and actual ROM angle (44°). (c), actual wrist extending (yellow curve) and desired (black curve) workspace trajectories, position, and actual ROM angle (25°). (d), the wrist relaxing position (zero position). (e), actual wrist radial deviation (blue curve) and desired (yellow curve) workspace trajectories and actual ROM angle (36°). (f) actual wrist ulnar deviation (blue

curve) and desired (yellow curve) workspace trajectory and actual ROM angle (49°).

Similarly, the wrist R/U experiment was conducted to evaluate and compare the wrist R/U joint's functional region with and without the proposed machine. In this experiment, the desired R/U ROM was selected from the control dashboard to be (0°–38°/0°–49°). Once the therapy was executed, the end-user performed wrist R/U motion with slow rpm as shown in Figure 38(d, e, f), which indicates; (1) the yellow curve, which describes the workspace trajectories without the proposed system; (2) the blue curve, which describes the real-time wrist R/U workspace trajectories induced by the proposed system.
Moreover, a graphical representation for wrist F/E and R/U ROM were created. The same applied the same previous approach in the finger F/E;. Figure 39(a) plots a comparative analysis between the desired and actual ROMs angle of the wrist F/E during the experiment's execution. It is straightforward to observe that the end-user is performing a single F/E wrist. The vertical axis stands for the wrist's angle, while the horizontal axis stands for the execution time. The graph consists of two curves: the solid blue curve demonstrates the desired ROM angle. While the orange dash curve illustrates the actual ROM angle of the wrist F/E. It is possible to note the similarities between the two ROMs. Similarly, Figure 39 (b) plots a graphical analysis that indicates comparison graphs between the desired and actual ROM angles of the wrist R/U during the experiment's execution. The solid blue curve is plotting the desired ROM angles. In comparison, the dashed orange curve is plotting the actual ROM angles.

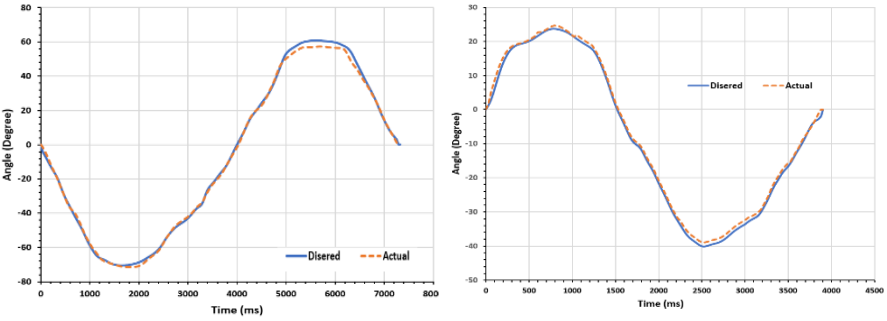

Figure 39: Continuous passive motion rehabilitation experiment of s typical. (a) wrist flexion/ extension joint; (b) wrist radial/ulnar deviation joint.

6.2.1. Wrist F/E and U/R result's Discussion

Although comparatively both trajectories in Figure 38 and ROM angles in Figure 39 (a, and b) are functionally matching towards each other, it is slightly observable that there is a slight error between them; it is worth noting as an error; the sum calculated RMSE was 0.984 mm. However, from Figure 39 (a, b) and Figure 39 (a), we can find a negligible observable error between the two ROMs and the workspace trajectories; the sum measured by root means square error RMSE of 1.1 4mm. Eventually, after the repeatable experimental tests, for the wrist therapies for both active and passive motions, the differences between the actual and the desired ROM were just a few millimetres for the finger's F/E and few degrees for the wrist F/E, R/U. The disparity in each measurement occurred primarily due to the mechanical frictions. However, as we have briefly explained, these differences do not affect the proposed system's training characteristics. Therefore, the results are sufficiently accurate in aspects of the stability and trajectory's alignment; the actual trajectory directly correlates to the desired trajectory, which meets the requirements of continuous passive motion training configurations.

6.3. Wrist uniaxial and boundary motions

the elliptical boundary motion can be actively performed by the participant. This type of motion is vital to increase wrist therapy efficiency. Wrist ellipse motion happens when the wrist seeks to rotate along the maximal border, and the hand makes an ellipse gradually. Figure 40 (a,b) depicts the trained elliptical motions for the left and right hands and the desired (blue dashed arcs) and actual values (the solid brown arcs). The proposed system needed to direct the wrist F/E and U/R deviations activated to perform the elliptical shape in the boundary motions. While Figure 40 (c) demonstrates a real-time captured active wrist elliptical training in which the participant actively holds the wrist handle and circulates it to perform a full elliptical shape. Additionally, the participant could actively achieve uniaxial motions with the help of the proposed system. When the patient holds the wrist handle and rotate the wrist horizontally (wrist R/U deviation) and vertically (wrist F/E deviation). From Figure 40 (d), this result was obtained from the left hand, in which the participant performs active motion, the F/E movements within (80 to -70 degrees). And wrist R/U deviation (40 to -30 degrees).

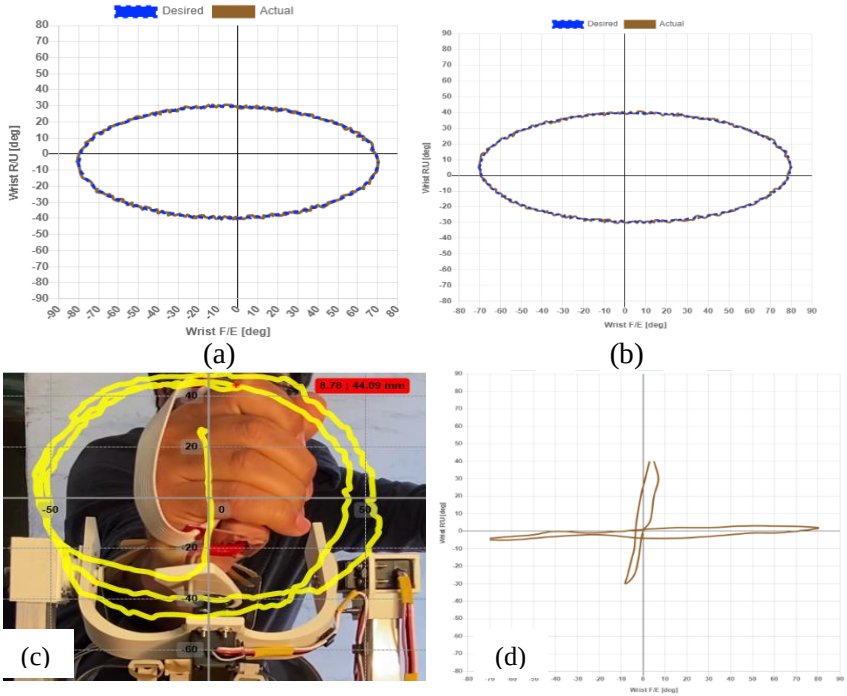

Figure 40: wrist elliptical motion: *Wrist uniaxial and boundary motions* (a), actual and desired elliptical motion of the right wrist; (b), actual and desired elliptical motion of the left wrist; (c), real-time results of elliptical motion. (d), wrist active uniaxial motions

6.4. Interactive game-based rehabilitation experimental results

The overall purpose of the developed game is to provide an engaging and amusing experience for individuals with impaired motor capability throughout the wrist that also includes a small amount of therapeutic exercise. To test how effectively the game's interactions function with the proposed system as well as to exhibit the proof of concept. The therapist can investigate the information and see how many times each participant has played the game. These data will be stored in the developed database, and it will list the maximum, highest game score, and date. The outcomes assessed by these test scores could be utilized to monitor and assess a patient's results throughout a period of time. Figure *41* present an example of game-based rehabilitation; while playing a game, patients interact with a virtual exporting and importing port, which receives their

responses and control inputs (hand movements) by changing its status. In this particular example game, the goal was set that the patient needs to move the white container (yellow highlighted) into the white ship. The patient needs to perform one wrist flexing to achieve that goal, then wrist radial deviation flexing one wrist extending. The exact process can be achieved to move other containers. In this way, the patient performing purely active wrist motion with different ROMs

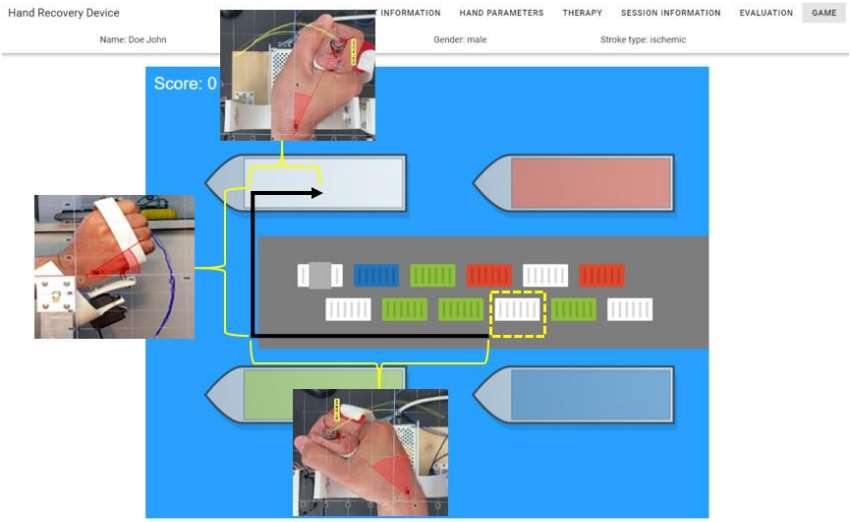

Figure 41: the developed game-based interactive rehabilitation

6.5. Subjective Evaluation Result with Healthy Participants

According to the feedback given by the healthy volunteers on the evaluation criteria of the proposed device based on a questionnaire proven to be safe to use and hence assuring the first observation to be fulfilled by the device which meets with the standard safety parameter. And the proposed system has achieved most of its aims and objectives. Another observation is based on the device's functionality in which users ranked it with the highest possible numbers, as shown from the bar graph illustrated in Figure 42.

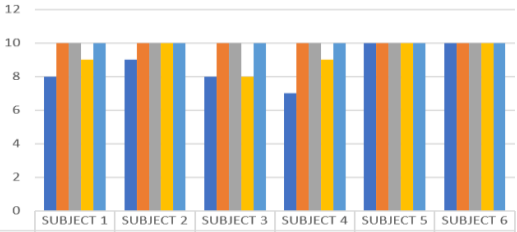

	SUBJECT 1	SUBJECT 2	SUBJECT 3	SUBJECT 4	SUBJECT 5	SUBJECT 6
(1= Uncomfortable, 10= Very Comfortable)	8	9	8	7	10	10
Device is Passive (YES, NO)	10	10	10	10	10	10
CPM motion Smoothness (1= Very Jerky, 10=Very Smooth)	10	10	10	10	10	10
Device forces the finger while applying resistance (1 = Very Strong, 10= Not felt)	9	10	8	9	10	10
Device's attachment painful (YES, NO)	10	10	10	10	10	10

Figure 42: Bar graph showing the Functionality and Safety measure of CPM device given by 06 healthy participants

Publications

1. **Almusawi, H.**, Husi, G.: Design and Development of Continuous Passive Motion (CPM) for Fingers and Wrist Grounded-Exoskeleton Rehabilitation System. *Appl. Sci.-Basel.* 11 (2), 1-23, 2021. Folyóirat-mutatók: Q1 Engineering (miscellaneous) (2019) IF: 2.474 (2019)

2. Saadah, A., **Almusawi, H.**, Husi, G.: Computing The Kinematics Study of a 6 DOF Industrial Manipulator Prototype by Matlab. *Recent Innov. Mechatron.* 7 (1), 1-5, 2020.

3. **Almusawi, H.**, Afghan, S., Husi, G.: Designing the Mechanical Parts of a Low-Cost Hand Rehabilitation CPM Device for Stroke Patients. In: Innovation, Engineering and Entrepreneurship. Eds.: José Machado, Filomena Soares, Germano Veiga, Springer, Cham, 60-66, 2019, (Lecture Notes in Electrical Engineering, ISSN 1876-1119 ; 505) ISBN: 9783319913346

4. Afghan, S., **Almusawi, H.**, Husi, G.: Simulating the Electrical Characteristics of Solar Panels based on Practical Single-Diode Equivalent Circuit Model: Analyzing the Influence of Environmental Parameters on Output Power.

In: Innovation, Engineering and Entrepreneurship. Eds.: José Machado, Filomena Soares, Germano Veiga, Springer, Cham, 67-74, 2019, (Lecture Notes in Electrical Engineering, ISSN 1876-1119 ; 505.) ISBN: 9783319913346

5. **Almusawi, H.**, Afghan, S., Husi, G.: Recent trends in robotic systems for upper-limb stroke recovery: A low-cost hand and wrist rehabilitation device.
In: 2nd International Symposium on Small-scale Intelligent Manufacturing Systems (SIMS), 2018, IEEE, Piscataway, 1-6, 2018. ISBN: 9781538644379

   All citations+mentions: 9, External citations: 8, Self citations: 1, Unhandled citations: 0

6. Afghan, S., **Almusawi, H.**, Husi, G.: Towards the self-powered Internet of Things (IoT) by energy harvesting: Trends and technologies for green IoT.
In: 2018 2nd International Symposium on Small-scale Intelligent Manufacturing Systems (SIMS), IEEE, Piscataway, 1-5, 2018. ISBN: 9781538644379

   All citations+mentions: 42, External citations: 42, Self citations: 0, Unhandled citations: 0

7. Afghan, S., **Almusawi, H.**, Husi, G.: Approximating the minimum output power for energy harvesting prototype: a case study of cell phone specifications = Minimális kimeneti teljesítmény meghatározása energy harvesting prototípushoz : egy esettanulmány mobiltelefon specifikációkra.
In: A XXII. Fiatal Műszakiak Tudományos Ülésszak előadásai = Proceedings of the XXII-th International Scientific Conference of Young Engineers. Szerk.: Bitay Enikő, Erdélyi Múzeum Egyesület, Kolozsvár, 55-58, 2017, (Műszaki Tudományos Közlemények, ISSN 2393-1280 ; 7.) ISBN: 9789634490180

8. **Almusawi, H.**, Afghan, S., Husi, G., Molnár, Z., Erdei, T.: Reviewing the notable progress of effective techniques in the development of stroke hand rehabilitation devices = A stroke-t kapott egyének

rehabilitációs eszközeiben jelentős fejlődést mutató hatékony technikák áttekintése.
In: A XXII. Fiatal Műszakiak Tudományos Ülésszak előadásai = Proceedings of the XXII-th International Scientific Conference of Young Engineers. Szerk.: Bitay Enikő, Erdélyi Múzeum Egyesület, Kolozsvár, 63-66, 2017, (Műszaki Tudományos Közlemények, ISSN 2393-1280 ; 7.) ISBN: 9789634490180

9. Molnár, Z., Erdei, T., **Almusawi, H.**, Husi, G.: Saját CNC prototípus rendszer mint IoT eszköz = Our Own CNC Prototype System as IoT Device.
In: A XXII. Fiatal Műszakiak Tudományos Ülésszak előadásai = Proceedings of the XXII-th International Scientific Conference of Young Engineers. Szerk.: Bitay Enikő, Erdélyi Múzeum Egyesület (EME), Kolozsvár, 295-298, 2017. ISBN: 9789634490180

10. Afghan, S., **Almusawi, H.**, Husi, G.: Simulating the electrical characteristics of a photovoltaic cell based on a single-diode equivalent circuit model.
In: Proceedings of the Annual Session of Scientific Papers "Imt Oradea - 2017", 25th-27th May, Oradea, Romania. Eds.: Calin Baban, Florin Sandu Blaga, Gavril Grebenisan, Alexandru-Viorel Pele, Mircea Teodor Pop, Alexandru Rus, Radu Catalin Tarca, University of Oradea Publishing House, Oradea, 181-186, 2017. ISBN: 9786061015375

11. Afghan, S., **Almusawi, H.**, Husi, G.: Simulating the electrical characteristics of a photovoltaic cell based on a single-diode equivalent circuit model.
Anal. Univ. Oradea. Fasc. Ing. Manag. Technol. 26 (1), 91-96, 2017.

12. Afghan, S., **Almusawi, H.**, Husi, G.: Simulating the electrical characteristics of a photovoltaic cell based on a single-diode equivalent circuit model.
MATEC Web Conf. 126 1-6, 2017.

All citations+mentions: 4, External citations: 4, Self citations: 0, Unhandled citations: 0

13. Afghan, S., **Almusawi, H.**, Jokhio, S., Husi, G.: Estimation of minimum output power threshold for energy harvesting module: an

inspection of battery and charging parameters of cell phones. In: Proceedings of 4th International Mechatronical Student Micro-Conference. Eds.: Adrienn Dineva, István Nagy, Óbudai Egyetem, Budapest, 56-71, 2016. ISBN: 9789634490166

14. **Almusawi, H.**, Afghan, S., Husi, G.: Technological advancements in stroke hand rehabilitation devices: a review. In: Proceedings of 4th International Mechatronical Student Micro-Conference. Eds.: Adrienn Dineva, István Nagy, Óbudai Egyetem, Budapest, 80-90, 2016. ISBN: 9789634490166

References

[1] W. S. Harwin, J. L. Patton, and V. R. Edgerton, "Challenges and Opportunities for Robot-Mediated Neurorehabilitation," *Proceedings of the IEEE*, vol. 94, no. 9, 2006, doi: 10.1109/jproc.2006.880671.

[2] W. Johnson, O. Onuma, M. Owolabi, and S. Sachdev, "Stroke: a global response is needed," *Bulletin of the World Health Organization*, vol. 94, no. 9, 2016, doi: 10.2471/blt.16.181636.

[3] J. Mackay and G. A. Mensah, *The atlas of heart disease and stroke*. World Health Organization, 2004.

[4] B. H. Dobkin, "Strategies for stroke rehabilitation," *The Lancet Neurology*, vol. 3, no. 9, pp. 528–536, Sep. 2004, doi: 10.1016/S1474-4422(04)00851-8.

[5] J. S. Tutak, "Virtual reality and exercises for paretic upper limb of stroke survivors," *Tehnički vjesnik*, vol. 24, no. Supplement 2, pp. 451–458, Sep. 2017, doi: 10.17559/TV-20161011143721.

[6] R. Nudo, "Adaptive plasticity in motor cortex: Implications for rehabilitation after brain injury," *Journal of rehabilitation medicine : official journal of the UEMS European Board of Physical and Rehabilitation Medicine*, vol. 35, pp. 7–10, Jun. 2003, doi: 10.1080/16501960310010070.

[7] "Stroke - Symptoms," *nhs.uk*, Oct. 24, 2017. https://www.nhs.uk/conditions/stroke/symptoms/ (accessed Apr. 09, 2021).

[8] G. Kwakkel, B. J. Kollen, J. van der Grond, and A. J. H. Prevo, "Probability of Regaining Dexterity in the Flaccid Upper Limb," *Stroke*, vol. 34, no. 9, 2003, doi: 10.1161/01.str.0000087172.16305.cd.

[9] C.-Y. Chu and R. M. Patterson, "Soft robotic devices for hand rehabilitation and assistance: a narrative review," *J NeuroEngineering*

Rehabil, vol. 15, no. 1, p. 9, Feb. 2018, doi: 10.1186/s12984-018-0350-6.
[10] B. Chen, B. Zi, Z. Wang, L. Qin, and W.-H. Liao, "Knee exoskeletons for gait rehabilitation and human performance augmentation: A state-of-the-art," *Mechanism and Machine Theory*, vol. 134, pp. 499–511, Apr. 2019, doi: 10.1016/j.mechmachtheory.2019.01.016.
[11] H. S. Lo and S. Q. Xie, "Exoskeleton robots for upper-limb rehabilitation: State of the art and future prospects," *Medical Engineering & Physics*, vol. 34, no. 3, pp. 261–268, Apr. 2012, doi: 10.1016/j.medengphy.2011.10.004.
[12] F. Ozkul and D. E. Barkana, "Upper-Extremity Rehabilitation Robot RehabRoby: Methodology, Design, Usability and Validation," *International Journal of Advanced Robotic Systems*, vol. 10, no. 12, 2013, doi: 10.5772/57261.
[13] "Bohannon RW, Smith MB. (1987) Interrater reliability of a modified Ashworth scale of muscle spasticity. Phys Ther 67:206-7.".
[14] J. Angeles and J. Angeles, *Fundamentals of robotic mechanical systems*, vol. 2. Springer, 2002.
[15] M. Lutz, *Programming Python*. O'Reilly Media, Inc., 2001.
[16] "MCP3424 - Analog to Digital Converters," *Microchip.com*, 2018. https://www.microchip.com/wwwproducts/en/mcp3424 (accessed Jan. 01, 2021).
[17] J. A. Balogun, C. T. Akomolafe, and L. O. Amusa, "Grip strength: Effects of testing posture and elbow position," *Archives of Physical Medicine and Rehabilitation*, vol. 72, no. 5, pp. 280–283, Apr. 1991, doi: 10.5555/uri:pii:000399939190241A.
[18] J. G. Andrews and Y. Youm, "A biomechanical investigation of wrist kinematics," *Journal of Biomechanics*, vol. 12, no. 1, pp. 83–93, Jan. 1979, doi: 10.1016/0021-9290(79)90012-5.
[19] M. A. Gull, S. Bai, and T. Bak, "A Review on Design of Upper Limb Exoskeletons," *Robotics*, vol. 9, no. 1, Art. no. 1, Mar. 2020, doi: 10.3390/robotics9010016.
[20] F. Ragazzo, "Review on Upper Limb Continuous Passive Motion Devices," *MATEC Web of Conferences*, vol. 53, p. 01062, 2016, doi: 10.1051/matecconf/20165301062.

UNIVERSITY AND NATIONAL LIBRARY
UNIVERSITY OF DEBRECEN
H-4002 Egyetem tér 1, Debrecen
Phone: +3652/410-443, email: publikaciok@lib.unideb.hu

Registry number: DEENK/373/2021.PL
Subject: PhD Publication List

Candidate: Husam Abdulkareem Almusawi
Doctoral School: Doctoral School of Informatics
MTMT ID: 10061313

List of publications related to the dissertation

Foreign language scientific articles in Hungarian journals (1)

1. Saadah, A., **Almusawi, H. A.**, Husi, G.: Computing The Kinematics Study of a 6 DOF Industrial Manipulator Prototype by Matlab.
Recent Innov. Mechatron. 7 (1), 1-5, 2020. EISSN: 2064-9622.
DOI: http://dx.doi.org/10.17667/riim.2020.1/8.

Foreign language scientific articles in international journals (1)

2. **Almusawi, H. A.**, Husi, G.: Design and Development of Continuous Passive Motion (CPM) for Fingers and Wrist Grounded-Exoskeleton Rehabilitation System.
Appl. Sci.-Basel. 11 (2), 1-23, 2021. ISSN: 2076-3417.
DOI: http://dx.doi.org/10.3390/app11020815
IF: 2.679 (2020)

Foreign language conference proceedings (4)

3. **Almusawi, H. A.**, Afghan, S. A., Husi, G.: Designing the Mechanical Parts of a Low-Cost Hand Rehabilitation CPM Device for Stroke Patients.
In: Innovation, Engineering and Entrepreneurship. Eds.: José Machado, Filomena Soares, Germano Veiga, Springer, Cham, 60-66, 2019, (Lecture Notes in Electrical Engineering, ISSN 1876-1119 ; 505) ISBN: 9783319913346

4. **Almusawi, H. A.**, Afghan, S. A., Husi, G.: Recent trends in robotic systems for upper-limb stroke recovery: A low-cost hand and wrist rehabilitation device.
In: 2nd International Symposium on Small-scale Intelligent Manufacturing Systems (SIMS), 2018, IEEE, Piscataway, 1-6, 2018. ISBN: 9781538644379

5. **Almusawi, H. A.**, Afghan, S. A., Husi, G., Molnár, Z., Erdei, T. I.: A stroke-t kapott egyének rehabilitációs eszközeiben jelentős fejlődést mutató hatékony technikák áttekintése = Reviewing the notable progress of effective techniques in the development of stroke hand rehabilitation devices.
In: A XXII. Fiatal Műszakiak Tudományos Ülésszak előadásai = Proceedings of the XXII-th International Scientific Conference of Young Engineers. Szerk.: Bitay Enikő, Erdélyi Múzeum Egyesület, Kolozsvár, 63-66, 2017, (Műszaki Tudományos Közlemények, ISSN 2393-1280 ; 7.) ISBN: 9789634490180

6. **Almusawi, H. A.**, Afghan, S. A., Husi, G.: Technological advancements in stroke hand rehabilitation devices: a review.
In: Proceedings of 4th International Mechatronical Student Micro-Conference. Eds.: Adrienn Dineva, István Nagy, Óbudai Egyetem, Budapest, 80-90, 2016. ISBN: 9789634490166

List of other publications

Foreign language scientific articles in international journals (1)

7. Afghan, S. A., **Almusawi, H. A.**, Husi, G.: Simulating the electrical characteristics of a photovoltaic cell based on a single-diode equivalent circuit model.
Anal. Univ. Oradea. Fasc. Ing. Manag. Technol. 26 (1), 91-96, 2017. ISSN: 1583-0691.

Hungarian conference proceedings (1)

8. Molnár, Z., Erdei, T. I., **Almusawi, H. A.**, Husi, G.: Saját CNC prototípus rendszer mint IoT eszköz = Our Own CNC Prototype System as IoT Device.
In: A XXII. Fiatal Műszakiak Tudományos Ülésszak előadásai = Proceedings of the XXII-th International Scientific Conference of Young Engineers. Szerk.: Bitay Enikő, Erdélyi Múzeum Egyesület (EME), Kolozsvár, 295-298, 2017, (Műszaki Tudományos Közlemények, ISSN 2393-1280 ; 7.) ISBN: 9789634490180

Foreign language conference proceedings (6)

9. Afghan, S. A., **Almusawi, H. A.**, Husi, G.: Simulating the Electrical Characteristics of Solar Panels based on Practical Single-Diode Equivalent Circuit Model: Analyzing the Influence of Environmental Parameters on Output Power.
In: Innovation, Engineering and Entrepreneurship. Eds.: José Machado, Filomena Soares, Germano Veiga, Springer, Cham, 67-74, 2019, (Lecture Notes in Electrical Engineering, ISSN 1876-1119 ; 505.) ISBN: 9783319913346

10. Afghan, S. A., **Almusawi, H. A.**, Husi, G.: Towards the self-powered Internet of Things (IoT) by energy harvesting: Trends and technologies for green IoT.
In: 2018 2nd International Symposium on Small-scale Intelligent Manufacturing Systems (SIMS), IEEE, Piscataway, 1-5, 2018. ISBN: 9781538644379

11. Afghan, S. A., **Almusawi, H. A.**, Husi, G.: Minimális kimeneti teljesítmény meghatározása energy harvesting prototípushoz: egy esettanulmány mobiltelefon specifikációkra = Approximating the minimum output power for energy harvesting prototype : a case study of cell phone specifications.
In: A XXII. Fiatal Műszakiak Tudományos Ülésszak előadásai = Proceedings of the XXII-th International Scientific Conference of Young Engineers. Szerk.: Bitay Enikő, Erdélyi Múzeum Egyesület, Kolozsvár, 55-58, 2017, (Műszaki Tudományos Közlemények, ISSN 2393-1280 ; 7.) ISBN: 9789634490180

12. Afghan, S. A., **Almusawi, H. A.**, Husi, G.: Simulating the electrical characteristics of a photovoltaic cell based on a single-diode equivalent circuit model.
MATEC Web Conf. 126, 1-6, 2017. EISSN: 2261-236X.
DOI: http://dx.doi.org/10.1051/matecconf/201712603002

13. Afghan, S. A., **Almusawi, H. A.**, Husi, G.: Simulating the electrical characteristics of a photovoltaic cell based on a single-diode equivalent circuit model. Utánközlés kiadói másodközlés,
In: Proceedings of the Annual Session of Scientific Papers "Imt Oradea - 2017", 25th-27th May, Oradea, Romania. Eds.: Calin Baban, Florin Sandu Blaga, Gavril Grebenisan, Alexandru-Viorel Pele, Mircea Teodor Pop, Alexandru Rus, Radu Catalin Tarca, University of Oradea Publishing House, Oradea, 181-186, 2017. ISBN: 9786061015375

14. Afghan, S. A., **Almusawi, H. A.**, Jokhio, S. H., Husi, G.: Estimation of minimum output power threshold for energy harvesting module: an inspection of battery and charging parameters of cell phones.
In: Proceedings of 4th International Mechatronical Student Micro-Conference. Eds.: Adrienn Dineva, István Nagy, Óbudai Egyetem, Budapest, 56-71, 2016. ISBN: 9789634490166

Total IF of journals (all publications): 2,679
Total IF of journals (publications related to the dissertation): 2,679

The Candidate's publication data submitted to the iDEa Tudóstér have been validated by DEENK on the basis of the Journal Citation Report (Impact Factor) database.